	Al
2.7	Cu
2.3	Li
0.12	Zr

2090 Al

1 **GENERAL**

This alloy was developed in the late 1970's in response to the desire for lighter aerospace structures following a steep rise in fuel prices. The 2090 alloy has approximately 8 percent lower density and a 10 percent higher elastic modulus than either 2024 or 7075, which it was designed to replace. Initially, it was hoped that direct substitution would be possible, with little change in aircraft fabrication procedures. Properly processed sheet products and other thin sections have strength and toughness combinations approaching those of 7075, coupled with lower fatigue crack growth rates. However, as the development programs progressed several important limitations were revealed (see 1.09) which indicate that direct substitution is possible in only limited applications.

At present 2090 is offered in two groups of tempers, a high-strength and relatively low toughness substitute for 7075-T6, and a medium-strength, damage-tolerant substitute for 2024-T3. Various tempers have been developed within these groups, most of which are not available. In most cases the heat treating and processing schedules are proprietary.

Two major aluminum producers offer the alloy in sheet and plate. Only one producer offers extrusions. Forgings have been made but their poor properties, compared with conventional aluminum alloys, have discouraged production.

1.01 **Commercial Designation**

2090.

1.02 **Alternate Designation**

None.

1.03 **Specifications**

An AMS for 2090-T83 is in preparation for issue in 1990.

1.031 Many of the tempers identified in the literature are experimental designations used by the producers, e.g., T8E41. Many of these are not yet registered. (See 3.011.)

1.04 **Composition**

1.041 Registered composition limits for alloy 2090, Table 1.041.

1.05 **Heat Treatment**

See 1.096 for health and safety considerations.

Salt bath heat treatment has been reported to have no additional safety problems if melting is avoided. (See 1.081.)

T81 temper: Solution heat treat 986 F for 1 hr, water quench, cold work 6%, age 24 hr at 374 F (13).

T83: Solution heat at 1020 F, water quench, 6% cold work, age 24 hr at 60 F.

Extended times at solution heat treatment temperatures may result in the loss of some lithium from the surface layers of the product.

1.06 **Hardness**

In addition to varying with time and aging temperature, the hardness of this alloy is markedly sensitive to the degree of cold work between quenching and aging.

1.061 Rockwell B hardness versus aging time at temperatures in the range 320 F to 455 F, Figure 1.061.

1.062 Rockwell B and E hardness of 2090 sheet in -T3 and -T8 condition, Table 1.062.

1.063 Maximum hardnesses in a superplastically formed component, Table 1.063.

1.064 Aging curves for a superplastically formed component at 320 F, Figure 1.064.

1.065 Aging curves for a superplastically formed component at 350 F, Figure 1.065.

1.066 Aging curves for a superplastically formed component at 375 F, Figure 1.066.

1.07 **Forms and Conditions Available**

All forms are available only from the producer. Sheet, 0.02 to 0.249 inch thick, bare and clad (9,14). Plate, 0.25 to 1.5 inch thick. Extrusions, in shapes producible from a 16-inch diameter billet (9).

1.08 **Melting and Casting Practices**

1.081 The presence of lithium in alloy 2090 complicates melting practices. It destroys the protective nature of the oxide film formed on molten aluminum, and causes rapid oxidation, with enhanced likelihood of oxide inclusions being entrapped in the alloy. The risk of explosions, particularly in the presence of moisture or rust, is high. Lithium also increases the rate of attack of the melt on refractories normally used to contain molten aluminum. Care should be taken to ensure that fluxes and salts are compatible with the molten alloy.

As lithium is a contaminant in most conventional alloys, scrap must be segregated to prevent its entry into the scrap cycle of conventional alloys (3).

1.09 **Special Considerations**

1.091 Commercial 2090 has an unrecrystallized grain structure. This structure is associated with the highest combination of strength and (LT and TL) toughness. However, this product possesses a high degree of anisotropy with the tensile strength at 45° to the rolling direction being about 15 to 20 percent lower than the strength in the longitudinal or transverse directions. This requires special design considerations.

1.092 The alloy possesses a pronounced laminar microstructure which results in low short-transverse tensile ductility and poor toughness for the SL and ST crack orientations. This laminar structure also can cause delaminations during shearing sheet or thin extruded sections. Spalling may also be encountered during machining.

1.093 In order to develop peak strength, the alloy requires more deformation after solution heat treatment than the conventional aluminum alloys. From 5 to 8 percent cold work is necessary to develop peak strength and toughness in aged 2090. In

	Al
2.7	Cu
2.3	Li
0.12	Zr

2090 Al

some fabrication processes such as forging, this may be impossible.

1.094 The alloy ages at moderately elevated service temperatures with significant increases in strength coupled with substantially reduced fracture toughness and a change in fracture mode from transgranular to intergranular.

1.095 The scrap from Al-Li alloys is a contaminant to the normal aluminum scrap cycle and must be segregated.

1.096 Health. Lithium compounds are poisonous if ingested, and these may be formed during melting or chemical processing. Carbonates or oxides that are formed on metal surfaces at high temperatures react with atmospheric moisture, perspiration, or water, to form caustic compounds that may cause mild chemical burns. Care should be taken in handling 2090 components that have previously been heated to high temperatures.

The fines generated during grinding, machining, forging, welding or melting are potentially irritating to the mucous membranes. The degree of irritation varies markedly between individuals (3).

1.097 Safety. See melting and casting, 1.081.

2 PHYSICAL AND CHEMICAL PROPERTIES

2.01 Thermal Properties

2.011 Melting range: 1042 to 1054 F (48).

2.012 Phase changes: alloy is subject to precipitation.

2.0121 Time-temperature-transformation diagrams.

2.013 Thermal conductivity: 48.2–53.4 Btu-ft/hr-ft-F (0.834–0.924 J/sec-cm^2-C/cm) (48).

2.014 Thermal expansion. Linear coefficient of thermal expansion: at 68 to 212 F: 9 x 10^{-6} in./in./F (48).

2.015 Specific heat. Specific heat at 212 F: 0.2873 Btu/lb-F (48).

2.016 Thermal diffusivity.

2.02 Other Physical Properties

2.021 Density: 0.093 lb/in.^{3}, 2.59 gm/cm^3 (1); 2.57 gm/cm^3 (48).

2.022 Electrical properties.

2.0221 Electrical conductivity. The electrical conductivity of 2090 is markedly less than conventional alloys. Sheet in solution heat treated condition (T3): 15.5–16.5% IACS; after stretching and aging to T8: 18.0–19.0% IACS (34).

2.023 Magnetic properties. Alloy is nonmagnetic.

2.024 Emissivity.

2.025 Damping capacity.

2.03 Chemical Environments

2.031 General corrosion.

2.0311 Exfolidation corrosion of 2090-T83 plate, Table 2.0311.

2.0312 Exfoliation of 2090 plate, Table 2.0312.

2.0313 Corrosion test comparison, 2090 plate, Table 2.0313.

2.0314 Accelerated corrosion tests of 0.5 inch plate of 2090, Table 2.0314.

2.032 Stress corrosion.

2.0321 Stress corrosion of 2090-T83 plate, effect of composition, Table 2.0321.

2.0322 Stress corrosion of 2090-T83 extrusion, effect of aging, Table 2.0322.

2.0323 Time to failure for 2090 1.5-inch plate in various environments, Table 2.0323.

2.0324 Stress corrosion data (time to failure) for 2090 sheet, Table 2.0324.

2.0325 Crevice corrosion of 2090 sheet, Table 2.0325.

2.0326 Stress corrosion crack growth rate for 2090 T-X extrusions in 3.5% NaCl, Figure 2.0326.

2.0327 Stress corrosion results for 2090-T81 plate in various environments, Table 2.0327.

2.0328 Stress corrosion crack growth rates in 3.5% NaCl for 2090-T81 and 7075-T61 plate tested in the SL direction, Figure 2.0328.

2.033 Alloy has been reported to react more than conventional alloys when impacted in liquid oxygen.

2.034 Hydrogen embrittlement.

2.0341 Effect of hydrogen charging on the mechanical properties of 2090 plate, Table 2.0341.

2.0342 Effect of hydrogen charging on the strength of 2090-T83 0.5-inch plate, Figure 2.0342.

2.0343 Effect of hydrogen charging on the fracture strain of 2090-T83 0.5-inch plate, Figure 2.0343.

2.04 Nuclear Environments

3 MECHANICAL PROPERTIES

3.01 Specified Mechanical Properties

3.011 Aluminum Association registered tempers, Table 3.011.

3.02 Mechanical Properties at Room Temperature

3.021 Tension.

3.0211 Stress strain curve for 2090-T83 sheet, Figure 3.0211.

3.0212 Tensile properties of 2090-T83 plate from two sources, Table 3.0212.

3.0213 Tensile properties of various 2090 product forms in the -T6 and underaged tempers, Table 3.0213.

3.0214 Tensile properties of 2090-T83 extrusion, Table 3.0214.

3.0215 Tensile properties of 2090-T3 sheet, Table 3.0215.

3.0216 Tensile properties of 2090-T31 and -T83 sheet, Table 3.0216.

3.0217 Tensile properties of 2090-T83 sheet, Table 3.0217.

3.0218 Tensile properties of superplastically formed 2090-T6 sheet, Table 3.0218.

3.0219 Strength-ductility relationships for 0.090-inch 2090 sheet in various tempers, Figure 3.0219.

3.02110 Yield strength as a function of orientation to the rolling direction for 2090-T83 and 7075-T6 sheet, Figure 3.02110.

3.02111 Yield strength as a function of stretching and aging at 375 F, Figure 3.02111.

3.02112 Yield strength and elongation as a function of cold work before aging in 2090-T6 hand forgings, Figure 3.02112.

3.02113 Transverse yield strength as a function of cold work before aging in 2090 extrusions, Figure 3.02113.

3.02114 Tensile properties as a function of cold work (rolling) before aging in 2090 sheet, Figure 3.02114.

3.02115	Effect of exposure at 150 F on the tensile properties of 2090 plate and extrusion. (See also Table 3.027211), Table 3.02115.
3.02116	Effect of exposure at 200 F on the tensile properties of 2090 sheet. (See also 3.02727), Figure 3.02116.
3.022	Compression.
3.0221	Compressive yield strength of 2090-T83 sheet, Table 3.0221.
3.0222	Proposed compressive yield design allowables for 2090-T83 sheet, Table 3.0222.
3.0223	Compressive stress-strain and tangent modulus curves for 2090-T83 sheet, Figure 3.0223.
3.023	Impact.
3.0231	Charpy-V results for 2090 plate cold worked various amounts and aged to equivalent strength, Table 3.0231.
3.024	Bending. Minimum bend radii for design, in multiples of sheet thickness (longitudinal direction): as quenched (W temper) = 1.5; -T3 = 3.0; -T6 = 5.0; -T8 = 5.5 (46).
3.025	Torsion and shear.
3.0251	Shear strength of 2090-T83 sheet, Table 3.0251.
3.0252	Design allowable shear strength for 2090-T83 sheet, F_{su} is 37 ksi (1).
3.026	Bearing.
3.0261	Bearing properties of 2090-T83 sheet, Table 3.0261.
3.0262	Proposed design allowable bearing strengths for 2090-T83 sheet, Table 3.0262.
3.027	Stress concentration.
3.0271	Notch properties.
3.0272	Fracture toughness. In most semi-fabricated forms, the alloy possesses a laminar structure with the planes being parallel to the surface and extending in the major working direction. This structure results in irregular crack paths for cracks orientated normal to the layers. For crack orientations parallel to the layers (SL and ST), the fracture toughness is relatively low, as might be expected (Table 3.02728). As illustrated previously (Figure 3.02110), the unrecrystallized product exhibits a texture resulting in a substantial decrease in the yield strength at 45 degrees to the rolling direction. The fracture toughness with this crack orientation (TL + 45) appears slightly higher than for the LT and TL orientations (Table 3.02728). Extended exposure at 150 F results in increases in yield strength (see Table 3.02115) and substantial reduction in fracture toughness (Table 3.027211). Fracture toughness of sheet products in aluminum alloys is frequently measured using ASTM E561 Practice for R-Curve Determination. Two measures of toughness are obtained from the load versus crack opening displacement record. The first, K_C, is described in ASTM B646, and is determined from the maximum load in the test record, and the corresponding crack length at the maximum load. The second, $K_{apparent}$ ($K_{app.}$) is not described in ASTM B646, but is widely used in the aircraft industry. It is calculated from the maximum load, and the initial crack length. On the same test, $K_{app.}$ values are always less than or equal to K_C values. These K values are geometry dependent, and may be useful only for comparative purposes.
3.02721	Fracture toughness values for 2090 sheet, Table 3.02721.
3.02722	Fracture toughness of damage tolerant 2090 sheet, Table 3.02722.
3.02723	Fracture toughness of 2090-T83 sheet, Table 3.02723.
3.02724	Fracture toughness of production 2090 sheet as a function of strength level, Figure 3.02724.
3.02725	Fracture toughness of 2090 peak-aged sheet, Table 3.02725.
3.02726	Fracture toughness of various 2090 forms, Table 3.02726.
3.02727	Effect of exposure for 0 to 6 weeks at 200 F on the unit propagation energy in a Kahn test for 2090 sheet, Figure 3.02727.
3.02728	Plane-strain fracture toughness for plate and extrusions from a cooperative test program, Table 3.02728.
3.02729	Plane-strain fracture toughness of 2090-T83 plate for several crack orientations, Figure 3.02729.
3.027210	Plane-strain fracture toughness of 0.5-inch 2090-T83 plate, Table 3.027210.
3.027211	Effect of exposure at 150 F on the fracture toughness of 2090 plate and extrusion, Table 3.027211.
3.03	**Mechanical Properties at Various Temperatures** (See also 4.031.)
3.031	Tension.
3.0311	Tensile properties of 2090-T83 sheet at room and cryogenic temperatures, Table 3.0311.
3.0312	Tensile properties of 0.25-inch 2090-T62 and -T83 plate as a function of temperature, Figure 3.0312.
3.0313	Effect of low test temperatures on the short transverse tensile strength of 2090-T81 plate, Figure 3.0133.
3.0314	Tensile properties of 2090-T6 sheet, Table 3.0314.
3.032	Compression.
3.033	Impact.
3.034	Bending.
3.035	Torsion and shear.
3.036	Bearing.
3.037	Stress concentration.
3.0371	Notch properties.
3.0372	Fracture toughness.
3.03721	R curves for 2090-T83 sheet at ambient and liquid nitrogen temperatures, Figure 3.03721.
3.03722	Effect of low test temperatures on the tensile yield strength and plane-strain fracture toughness of 2090-T81 plate, Figure 3.03722.
3.03723	Kahn tear test toughness (LT) of 2090-T6 and -T81 at ambient and cryogenic temperatures, Table 3.03723.
3.038	Combined properties.
3.04	**Creep and Creep Rupture Properties**
3.05	**Fatigue Properties**
3.051	Conventional fatigue properties.
3.0511	Fatigue life of 2090-T83 0.5-inch plate in fully reversed bending, Figure 3.0511.
3.052	Fatigue crack propagation. Fatigue crack propagation rates of 2090 and other Al-Li alloys in tension loading appear to be lower than those of the 2XXX and 7XXX alloys. This advantage is in part due to crack tip shielding associated with irregular crack paths and the resulting roughness induced crack closure forces acting on relatively

Al
2.7 Cu
2.3 Li
0.12 Zr

2090 Al

	Al
2.7	Cu
2.3	Li
0.12	Zr

2090 Al

long cracks, but these forces are absent or greatly reduced for very short cracks (Figure 3.0524). The downside of this behavior is the relatively poor performance of Al-Li alloys in compression-dominated, variable amplitude spectra loading. This is illustrated by the reinitiation of cracks at crack tip stress intensity threshold values (K_{th}) when compression loads are applied (Figure 3.0525). Crack orientation effects are pronounced in this alloy with the SL and LT + 45-degree orientations showing the highest growth rates and the lowest K_{th} values (Figure 3.0523). Overaging for long times at 325 F leads to an increase in fatigue crack growth rates (Figure 3.0524).

3.0521 Fatigue crack growth curves for 0.5-inch 2090-T83 plate showing the effect of heterogeneity, Figure 3.0521.

3.0522 Fatigue crack growth rate for 0.5-inch 2090-T83 plate in air and in 3.5% NaCl, Figure 3.0522.

3.0523 Fatigue crack growth rates for 2090-T83 plate showing the effects of crack orientation and K_{th} values, Figure 3.0523.

3.0524 Fatigue crack growth rates for long and very short cracks in 2090 0.5-inch plate, showing the effects of aging time, Figure 3.0524.

3.0525 Crack growth at a constant value of $K = \Delta K_{th}$, following various compression overloads, Figure 3.0525.

3.0526 Fatigue crack growth rate of 2090-T83 0.5-inch plate in humid air, Figure 3.0526.

3.06 **Elastic Properties**

3.061 Elastic moduli of 2090-T83 plate, Table 3.061.

3.062 Elastic moduli of 2090-T83 sheet for several testing directions, Table 3.062.

3.063 Anisotropy of Young's Modulus in 2090-T83 sheet, Figure 3.063.

3.064 Anisotropy of Young's Modulus in 2090-T83 sheet, effect of aging at 325 F, Figure 3.064.

3.065 Anisotropy of Young's Modulus in 2090-T83 sheet and extrusion, effect of thickness, Figure 3.065.

3.066 Anisotropy of Poisson's Ratio in 2090-T83 plate, Figure 3.066.

3.067 Anisotropy of shear modulus in 2090 sheet, effect of aging at 325 F (163 C), Figure 3.067.

4 FABRICATION

4.01 **Forming**

An advantage of 2090 is that it is relatively stable in the solution-heat-treated and quenched condition. Unlike 2024, it can be stored at room temperature for up to a year before forming. It has good ductility, but less than 2024-O temper, and can be low-temperature aged to final properties without the need for high temperature heat treatment and consequent distortion.

4.011 Flow stress versus strain rate for 2090 sheet superplastically formed at 985 F, Figure 4.011.

4.02 **Machining and Grinding**

For health hazards associated with fines, see 1.091 above.

4.03 **Joining**

4.031 Welding. There has been only a limited amount of welding experience with the 2090 alloy. Data are available for variable polarity plasma arc (VPPA) gas-tungsten-arc (GTA), and electron beam welds in both sheet and plate (49). Acceptable fillers have been reported as 4043, 4047, 4245, 2319 and 5556, with 2319 and 5556 having the least hot cracking susceptibility (49). As-welded (VPPA) tensile properties can be considerably improved by solution treating and aging to the T62 condition with a joint efficiency of essentially 100 percent at room temperature and about 80 percent at -423 F (Table 4.0312). It is important that the surface of material to be welded is free of contaminants. This can be assured either by hand scraping or milling to remove about 0.01-inch of surface material. Moisture should be minimized as in the welding of any aluminum alloy.

4.0312 Tensile properties of VPPA-welded 2090-T83 sheet at low temperatures for several post-weld heat treatments, Table 4.0312.

4.0313 Tensile properties of 2090-T83 sheet welded by VPPA and GTA processes, Table 4.0313.

4.0314 Comparison of parent metal and weld metal tensile properties for 2090 sheet and 2219 plate, Table 4.0314.

4.0315 Tensile properties at cryogenic temperatures for 2090-T83 sheet welds, Table 4.0315.

4.0316 Fracture toughness as a function of low temperatures for parent metal and VPPA welds, Figure 4.0316.

4.0317 Tensile properties of welded and unwelded 2090-T83 plate as a function of temperature, Table 4.0317.

4.04 **Surface Treatment**

No difficult problems are reported in anodizing, surface treating, or chemical milling 2090 components.

REFERENCES

1 Minutes, Military Handbook 5 Committee, 77th Meeting (1989).

2 Aluminum Association Registered Temper Designations (August, 1989).

3 Aluminum Association Publication T4, "The Safety, Health and Recycling Aspects of Aluminum-Lithium Alloys", The Aluminum Association, Washington, DC.

4 Colvin, E. L., "Exfoliation and Stress Corrosion Cracking Performance of Al-Li Alloys", p 237 in "Aluminum Lithium Alloys, Design, Development and Applications Update", Symposium Proceedings, ASM International, Los Angeles, CA, R. J. Kar, S. P. Agrawal, and W. E. Quist, Eds. (March, 1987).

5 Waldman, J., Mahapatra, R., and Neu, C., "Aluminum Lithium Alloys for Navy Aircraft", p 341 in "Aluminum Lithium Alloys, Design, Development and Applications Update", Symposium Proceedings, ASM International, Los Angeles, CA, R. J. Kar, S. P. Agrawal, and W. E. Quist, Eds. (March, 1987).

6 Reynolds, M. J., Henshall, C. A., and Wadsworth, J., "Superplastic Forming Characteristics and Properties of Aluminum Lithium Alloys", p 387 in "Aluminum Lithium Alloys, Design, Development and Applications Update", Symposium Proceedings, ASM International, Los Angeles, CA, R. J. Kar, S. P. Agrawal, and W. E. Quist, Eds. (March, 1987).

7 Quist, W. E., Hyman, M., Gane, D. H., and Badger, D. V., "Forming Characteristics of Aluminum Lithium Alloys", p 401 in "Aluminum Lithium Alloys, Design, Development and Applications Update", Symposium Proceedings, ASM International, Los Angeles, CA, R. J. Kar, S. P. Agrawal, and W. E. Quist, Eds. (March, 1987).

8 Venkatesware, K. T., Yu, R. W., and Ritchie, R. O., "Mechanisms of Fatigue Crack Propagation in Commercial Aluminum Lithium Alloys", p 173 in "Aluminum Lithium Alloys, Design, Development and Applications Update", Symposium Proceedings, ASM International, Los Angeles, CA, R. J. Kar, S. P. Agrawal, and W. E. Quist, Eds. (March, 1987).

9 Bretz, P. E., "Alithalite Alloys: 1987 Update", p 1 in "Aluminum Lithium Alloys, Design, Development and Applications Update", Symposium Proceedings, ASM International, Los Angeles, CA, R. J. Kar, S. P. Agrawal, and W. E. Quist, Eds. (March, 1987).

10 Dorward, R. C., "Al-Li Development at Kaiser Aluminum", p 155 in "Aluminum Lithium Alloys, Design, Development and Applications Update", Symposium Proceedings, ASM International, Los Angeles, CA, R. J. Kar, S. P. Agrawal, and W. E. Quist, Eds. (March, 1987).

11 Blackburn, L., Casada, W., Colvin, G., Shiftler, G., and Starke, E., "The Effect of Processing on the Strength and Fracture Behavior of Aluminum Lithium Alloys", p 187 in "Aluminum Lithium Alloys, Design, Development and Applications Update", Symposium Proceedings, ASM International, Los Angeles, CA, R. J. Kar, S. P. Agrawal, and W. E. Quist, Eds. (March, 1987).

12 Monhaghegh, M., Zafari, F., Pada, C. S., and Lin, F., "Property Trends for 2091 and 2090 Sheet", p 237 in "Aluminum Lithium Alloys, Design, Development and Applications Update", Symposium Proceedings, ASM International, Los Angeles, CA, R. J. Kar, S. P. Agrawal, and W. E. Quist, Eds. (March, 1987).

13 Glazer, J., and Morris, J. W., "The Strength-Toughness Relationships at Cryogenic Temperatures in Aluminum Lithium Alloy Plate", p 1471 in "Aluminum-Lithium Alloys", Proc. Fifth International Al-Li Conference, Williamsburg, VA, T. H. Sanders and E. A. Starke, Eds., Materials and Component Engineering Publications, Ltd., Birmingham, UK (March, 1989).

14 Kaiser Aluminum and Chemical Corporation, Data Sheets on 2090 Alloy (January, 1988).

15 Pao, P. S., Imam, M. A., Cooley, L. A., and Yoder, G. R., "Corrosion Fatigue Crack Growth in Al-Li Alloy 2090", p 1125 in "Aluminum-Lithium Alloys", Proc. Fifth International Al-Li Conference, Williamsburg, VA, T. H. Sanders and E. A. Starke, Eds., Materials and Component Engineering Publications, Ltd., Birmingham, UK (March, 1989).

16 Tobler, R. L., Han, J. K., Ma, L., Walsh, R. P., and Reed, R. P., "Tensile, Fracture, and Fatigue Properties of Notched Aluminum Alloy Sheets at Liquid Nitrogen Temperatures", p 1115 in "Aluminum-Lithium Alloys", Proc. Fifth International Al-Li Conference, Williamsburg, VA, T. H. Sanders and E. A. Starke, Eds., Materials and Component Engineering Publications, Ltd., Birmingham, UK (March, 1989).

17 Yoder, G. R., Pao, P. S., Imam, M. A., and Cooley, L. A., "Micromechanisms of Fatigue Fracture in Al-Li Alloy 2090", p 103 in "Aluminum-Lithium Alloys", Proc. Fifth International Al-Li Conference, Williamsburg, VA, T. H. Sanders and E. A. Starke, Eds., Materials and Component Engineering Publications, Ltd., Birmingham, UK (March, 1989).

18 Rioja, R. J., Bretz, P. E., Sawtell, R. R., Hunt, W. H., and Ludwiczac, E. A., "Aluminum Alloys: Their Physical and Mechanical Properties", EMAS Ltd., Warley, UK, E. A. Starke and T. H. Sanders, Eds. (1986).

19 Crookes, R., and Mitchell, M. R., "The Fracture of 2090 Plate in Bending Fatigue", p 1023 in "Aluminum-Lithium Alloys", Proc. Fifth International Al-Li Conference, Williamsburg, VA, T. H. Sanders and E. A. Starke, Eds., Materials and Component Engineering Publications, Ltd., Birmingham, UK (March, 1989).

20 Venkateswara Rao, K. T., Piascik, R. S., Gangloff, R. P., and Ritchie, R. O., "Fatigue Crack Propagation in Aluminum Lithium Alloys", p 955 in "Aluminum-Lithium Alloys", Proc. Fifth International Al-Li Conference, Williamsburg, VA, T. H. Sanders and E. A. Starke, Eds., Materials and Component Engineering Publications, Ltd., Birmingham, UK (March, 1989).

21 Rooney, W. D., Papazian, J. M., Balmuth, E. S., Davis, R. C., and Adler, P. N., "Elastic Anisotropy in Al-Li Alloys", p 799 in "Aluminum-Lithium Alloys", Proc. Fifth International Al-Li Conference, Williamsburg, VA, T. H. Sanders and E. A. Starke, Eds., Materials and Component Engineering Publications, Ltd., Birmingham, UK (March, 1989).

22 Bretz, P. E., "Low Density Aluminum Technology", p 74 in "Aluminum-Lithium, Development, Application, and Superplastic Forming", Proc. ASM Symposium, Los Angeles, CA, S. P. Agrawal and R. J. Kar, Eds., ASM, Metals Park, OH (1986).

23 Cassada, W. A., Shiflet, G. J., and Starke, E. A., "The Precipitation, Deformation, and Fracture Behavior of Aluminum-Lithium Alloys", p 2 in "Aluminum-Lithium, Development, Application, and Superplastic Forming", Proc. ASM Symposium, Los Angeles, CA, March, 1986, S. P. Agrawal and R. J. Kar, Eds., ASM, Metals Park, OH (1986).

24 Glazer, J., and Morris, J. W., "Thermomechanical Processing of Two Phase Al-Cu-Li-Zr Alloys", p 191 in "Aluminum-Lithium Alloys 3", Proc. Symposium, The Institute of Metals, Oxford, UK, July, 1985, C. Baker, P. J. Gregson, S. J. Harris, and C. J. Peel, Eds., The Institute of Metals, London (1986).

	Al
2.7	Cu
2.3	Li
0.12	Zr

2090 Al

	Al
2.7	Cu
2.3	Li
0.12	Zr

2090 Al

25 Skillingberg, M. H., and Ashton, R. F., "Processing and Performance of Al-Li-Cu-X Extrusions", p C3-179 in "4th International Aluminum-Lithium Conference", Conference Proceedings, June, 1987, Paris, France, G. Champier, B. Dubost, D. Miannay, and L. Sabetay, Eds., Journal de Physique, Les Ulis, France (1987).

26 Papazian, J. M., Bott, G. G., and Shaw, P., "Influence of Forming in the T3 Condition on Properties of 2090-T8X, 2091-T8X, and 8090-T8X", p C3-231 in "4th International Aluminum-Lithium Conference", Conference Proceedings, June, 1987, Paris, France, G. Champier, B. Dubost, D. Miannay, and L. Sabetay, Eds., Journal de Physique, Les Ulis, France (1987).

27 Lippold, J. C., "Weldability of Commercial Aluminum-Lithium Alloys", p 1365 in "Aluminum-Lithium Alloys", Proc. Fifth International Al-Li Conference, Williamsburg, VA, March, 1989, T. H. Sanders and E. A. Starke, Eds., Materials and Component Engineering Publications, Ltd., Birmingham, UK (1989).

28 Zacharia, T., David, S. A., Vitek, J. M., and Martukanitz, R. P., "Weldability and Microstructure Characterization of Al-Li Alloys", p 1387 in "Aluminum-Lithium Alloys", Proc. Fifth International Al-Li Conference, Williamsburg, VA, March, 1989, T. H. Sanders and E. A. Starke, Eds., Materials and Component Engineering Publications, Ltd., Birmingham, UK (1989).

29 Kramer, L. S., Heubaum, F. H., and Pickens, J. R., "The Weldability of High-Strength Al-Cu-Li Alloys", p 1415 in "Aluminum-Lithium Alloys", Proc. Fifth International Al-Li Conference, Williamsburg, VA, March, 1989, T. H. Sanders and E. A. Starke, Eds., Materials and Component Engineering Publications, Ltd., Birmingham, UK (1989).

30 Marsico, T. A., and Kossowsky, R., "Physical Properties of Laser-Welded Aluminum-Lithium Alloy 2090", p 1447 in "Aluminum-Lithium Alloys", Proc. Fifth International Al-Li Conference, Williamsburg, VA, March, 1989, T. H. Sanders and E. A. Starke, Eds., Materials and Component Engineering Publications, Ltd., Birmingham, UK (1989).

31 Griffee, C. C., Jensen, G. A., and Reinhart, T. L., "Factors Influencing the Quality and Properties of Aluminum Alloy Welds", p 1425 in "Aluminum-Lithium Alloys", Proc. Fifth International Al-Li Conference, Williamsburg, VA, March, 1989, T. H. Sanders and E. A. Starke, Eds., Materials and Component Engineering Publications, Ltd., Birmingham, UK (1989).

32 Pao, P. S., Cooley, L. A., Imam, M. A., and Yoder, G. R., "Fatigue Crack Growth in 2090 Al-Li Alloy", pp 1455 to 1460, Scripta Metallurgica, Vol 23, No. 8.

33 Buscemi, C. D., and Chin, E.S.C., "Characterization of X2090 Al-Li Alloy", Report MTL-TR-88-26, U.S. Army Laboratory Command, Materials Technology Laboratory, Watertown, Mass. (September, 1988).

34 Dorward, R. C., Kaiser Aluminum and Chemical Corp., Pleasanton, CA, personal communication.

35 Kaiser Aluminum and Chemical Corp., Data Sheets, Vol 2 (1988).

36 Moran, J. P., and Stoner, G. E., "Solution Chemistry Effects on the Stress Corrosion Behavior of Alloy 2090 and 2034", p 1187 in "Aluminum-Lithium Alloys", Proc. Fifth International Al-Li Conference, Williamsburg, VA, March, 1989, T. H. Sanders and E. A. Starke, Eds., Materials and Component Engineering Publications, Ltd., Birmingham, UK (1989).

37 Bavarian, B., Becker, J., Parikh, S. N., and Zamanzadeh, M., "Localized Corrosion of 2090 and 2091 Al-Li Alloy", p 1227 in "Aluminum-Lithium Alloys", Proc. Fifth International Al-Li Conference, Williamsburg, VA, March, 1989, T. H. Sanders and E. A. Starke, Eds., Materials and Component Engineering Publications, Ltd., Birmingham, UK (1989).

38 Colvin, E. L., and Murtha, S. J., "Exfoliation Corrosion Testing of Al-Li Alloys 2090 and 2091", p 1251 in "Aluminum-Lithium Alloys", Proc. Fifth International Al-Li Conference, Williamsburg, VA, March, 1989, T. H. Sanders and E. A. Starke, Eds., Materials and Component Engineering Publications, Ltd., Birmingham, UK (1989).

39 Meletis, E. I., and Huang, W., "Pre-Exposure Embrittlement in Al-Li-Cu-Zr Alloys", p 1309 in "Aluminum-Lithium Alloys", Proc. Fifth International Al-Li Conference, Williamsburg, VA, March, 1989, T. H. Sanders and E. A. Starke, Eds., Materials and Component Engineering Publications, Ltd., Birmingham, UK (1989).

40 Shin, K. S., Kim, S. S., and Lee, E. W., "Hydrogen Embrittlement of a 2090 Al-Li Alloy", p 1319 in "Aluminum-Lithium Alloys", Proc. Fifth International Al-Li Conference, Williamsburg, VA, March, 1989, T. H. Sanders and E. A. Starke, Eds., Materials and Component Engineering Publications, Ltd., Birmingham, UK (1989).

41 Rivet, F. C., and Swanson, R. E., "Influence of Dissolved Hydrogen on Aluminum-Lithium Alloy Fracture Behavior", p 1329 in "Aluminum-Lithium Alloys", Proc. Fifth International Al-Li Conference, Williamsburg, VA, March, 1989, T. H. Sanders and E. A. Starke, Eds., Component Engineering Publications, Ltd., Birmingham, UK (1989).

42 Griffee, C. C., Jensen, G. A., and Reinhart, T. L., "Factors Influencing the Quality and Properties of Al-Li Alloy Welds", p 1425 in "Aluminum-Lithium Alloys", Proc. Fifth International Al-Li Conference, Williamsburg, VA, March, 1989, T. H. Sanders and E. A. Starke, Eds., Materials and Component Engineering Publications, Ltd., Birmingham, UK (1989).

43 Kerr, J. R., and Merino, R. E., "Cryogenic Properties of VPPA Welded Aluminum-Lithium Alloys", p 1491 in "Aluminum-Lithium Alloys", Proc. Fifth International Al-Li Conference, Williamsburg, VA, March, 1989, T. H. Sanders and E. A. Starke, Eds., Materials and Component Engineering Publications, Ltd., Birmingham, UK (1989).

44 Venkateswara Rao, K. T., and Ritchie, R. O., "Influence of Extrinsic Crack Deflection and Delamination Mechanisms on the Cryogenic Toughness of Al-Li Alloy 2090; Behavior in Plate

(T81) vs. Sheet (T83) Material", p 1501 in "Aluminum-Lithium Alloys", Proc. Fifth International Al-Li Conference, Williamsburg, VA, March, 1989, T. H. Sanders and E. A. Starke, Eds., Materials and Component Engineering Publications, Ltd., Birmingham, UK (1989).

45 Verzasconi, S. L., and Morris, J. W., "Cryogenic Mechanical Properties of Low Density Superplastically Formable Al-Li Alloys", p 1523 in "Aluminum-Lithium Alloys", Proc. Fifth International Al-Li Conference, Williamsburg, VA, March, 1989, T. H. Sanders and E. A. Starke, Eds., Materials and Component Engineering Publications, Ltd., Birmingham, UK (1989).

46 Tuegel, E. J., Vasey-Glandon, V. M., Pruitt, M. O., and Sankaran, K. K., "Forming of Aluminum Lithium Sheet for Fighter Aircraft Applications"; p 1597 in "Aluminum-Lithium Alloys", Proc. Fifth International Al-Li Conference, Williamsburg, VA, March, 1989, T. H. Sanders and E. A. Starke, Eds., Materials and Component Engineering Publications, Ltd., Birmingham, UK (1989).

47 Huang, J. C., and Ardell, A. J., "Microstructural Development in Two Al-Li-Cu Alloys", p 455 in "Aluminum-Lithium Alloys 3", Proc. Symposium The Institute of Metals, Oxford, UK, July, 1985, C. Baker, P. J. Gregson, S. J. Harris, and C. J. Peel, Eds., The Institute of Metals, London (1986).

48 Spiropoulos, P. T., "Thermomechanical Processing of an Al Alloy 2090 for Grain Refinement and Superplasticity", Thesis, December, 1987, Naval Postgraduate School, Monterey, CA (1987).

49 Bucci, R. J., Malcom, R. C., Colvin, E. L., Murtha, S. J., and James, R. S., "Cooperative Test Program for the Evaluation of Engineering Properties of Al-Li Alloy 2090-TX Sheet, Plate, and Extrusion Products", Aluminum Co. of America, NSWC-TR 89-06 (September 15, 1989).

Al
2.7 Cu
2.3 Li
0.12 Zr

2090 Al

Alloy	2090	
	Percent	
Element	Min	Max
Si	–	0.10
Fe	–	0.12
Cu	2.4	3.0
Mn	–	0.05
Mg	–	0.25
Cr	–	0.05
Zn	–	0.10
Li	1.9	2.6
Zr	0.08	0.15
Ti	–	0.15
Others		
Each	–	0.05
Total	–	0.15

TABLE 1.041. REGISTERED COMPOSITION LIMITS FOR ALLOY 2090 (2)

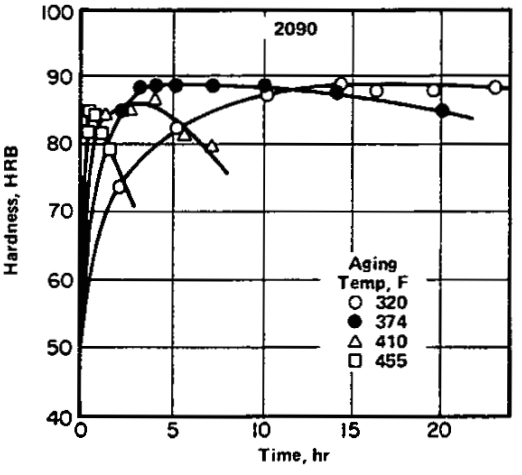

FIGURE 1.061. ROCKWELL B HARDNESS VERSUS AGING TIME AT TEMPERATURES IN THE RANGE 320 F TO 455 F (47)

	Al
2.7	Cu
2.3	Li
0.12	Zr

2090 Al

Alloy	2090		
Form	Sheet		
Gauge	0.063 in. and 0.10 in.		
Temper	-T3	Stretch,	-T8
Hardness	Rockwell E	percent	Rockwell B
	87.2	0	76.6
	95.1	1	84.7
	91.7	2.25	82.1
	95.3	3	85.5
	92.1	3.5	83.3
	90.5	5	85.9

TABLE 1.062. ROCKWELL B AND E HARDNESS OF 2090 SHEET IN -T3 AND -T8 CONDITION (34)

Alloy	2090					
Temper	T6					
Form	Superplastically Formed Sheet					
Aging Temperature, F	320		350		375	
Thickness, in.	Maximum Hardness, HRB	Time, hr	Maximum Hardness, HRB	Time, hr	Maximum Hardness, HRB	Time, hr
0.02	70	128	64	64	66	8
0.03	68	128	65	128	67	8–16
0.045	74	128	69	64	75	8–16
0.075	80	128	75	128	79	16
0.075 (Flange, as-received)	79	32	74	64	75	2–4

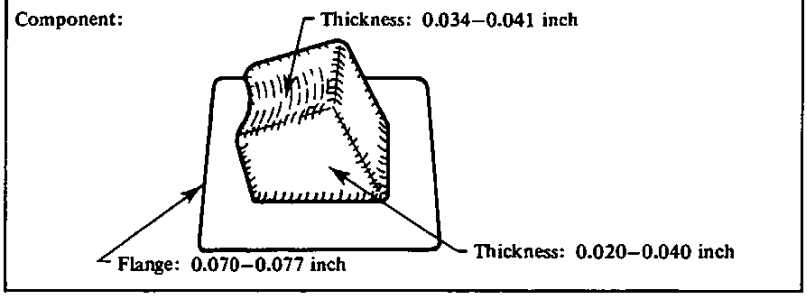

TABLE 1.063. MAXIMUM HARDNESS IN A SUPERPLASTICALLY FORMED COMPONENT (6)

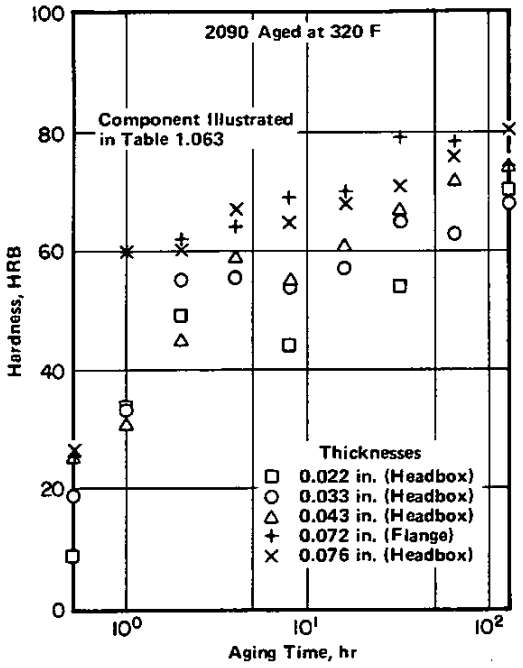

FIGURE 1.064. AGING CURVES FOR A SUPERPLASTICALLY FORMED COMPONENT AT 320 F (6)

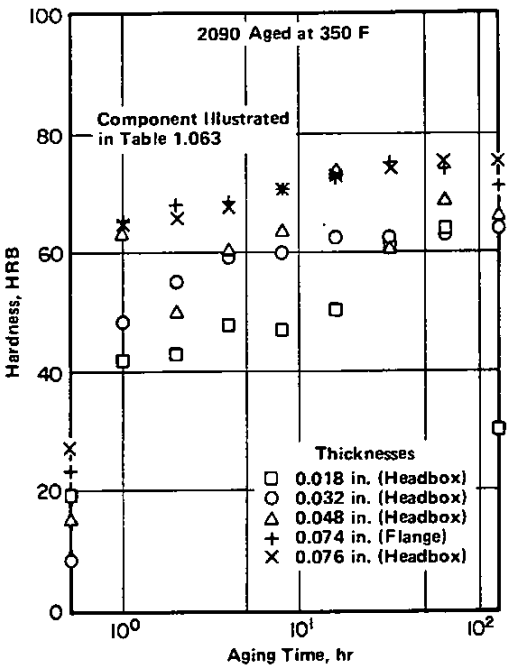

Al	
2.7	Cu
2.3	Li
0.12	Zr

2090 Al

FIGURE 1.065. AGING CURVES FOR A SUPERPLASTICALLY FORMED COMPONENT AT 350 F (6)

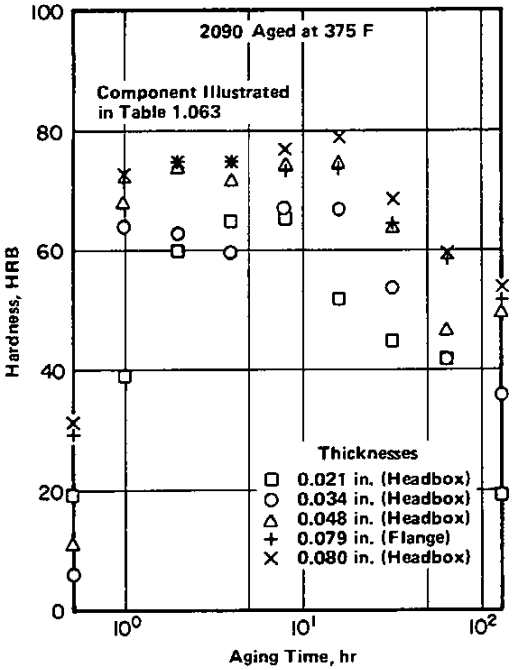

FIGURE 1.066. AGING CURVES FOR A SUPERPLASTICALLY FORMED COMPONENT AT 375 F (6)

Al
2.7 Cu
2.3 Li
0.12 Zr

2090 Al

Alloy			2090				
Temper			T83				
Form			Plate				
Composition, weight percent			Thickness,	Corrosion Exposure			
				EXCO[a]	MASTMAASIS[b]	Point Judith	
Li	Cu	Zr	in.	2 days	2 weeks	Months	Rating
2.2	2.5	0.12	0.25	EB[c]	p[c]	22	N[c]
2.2	3.0	0.12	0.25	EC	p	22	N
2.5	2.5	0.12	0.25	EC	p	22	N
2.5	3.0	0.12	0.25	EC	p	22	N
2.2	2.5	0.12	1.0	EA	p	22	N
2.2	3.0	0.12	1.0	EA	p	22	N
2.5	2.5	0.12	1.0	EA	p	22	N
2.5	3.0	0.12	1.0	EA	p	22	N

Note: These samples represent efforts to study the effects of composition variation on the properties of 2090. The panels have suffered no exfoliation in either MASTMAASIS or the Point Judith seacoast atmosphere, but EXCO attacked the 0.25 inch thick plate severely. Composition did not influence the results; the difference in EXCO ratings was probably caused by a more directional grain structure in the thinner plate.

(a) Total immersion in 4N, NaCl + 0.5N, KNO_3 + 0.1N, HNO_3 solution for 48 hours – ASTM Method G34-86.
(b) Exposure to acetic acid acidified salt spray, ASTM Method G85, Annex 2.
(c) Ratings according to ASTM Method G34-72: p = pitting and E = exfoliation; severity is denoted by the letter A, B, or C in increasing severity.

TABLE 2.0311. EXFOLIATION CORROSION OF 2090-T83 PLATE (4)

Alloy			2090					
Composition, weight percent					Corrosion Exposure			
				Temper,	EXCO[a],	MASTMAASIS[b],	Point Judith	
Li	Cu	Zr	Product	hr/temp, F	2 days	2 weeks	Months	Rating
2.0	3.0	0.12	1-in. Thick	-T3	N[c]	–	30	N
				8/300 (U)	EA	–	30	N
				16/325 (U)	N	–	30	N
				48/325 (O)	EB	–	30	N

Note: (U) underaged, (P) near peak-aged, (O) overaged.

(a) Total immersion in 4N, NaCl + 0.5N, KNO_3 + 0.1N, HNO_3 solution for 48 hours – ASTM Method G34-86.
(b) Exposure to acetic acid acidified salt spray, ASTM Method G85, Annex 2.
(c) Ratings according to ASTM Method G34-72: p = pitting, and E = exfoliation; severity is denoted by the letter A, B, or C in increasing severity.

TABLE 2.0312. EXFOLIATION OF 2090 PLATE (4)

Alloy			2090					
Temper			T83					
Form			Plate					
Composition				Gauge,	Temper,	EXCO[a],	MAST.[b],	Point Judith
Li	Cu	Zr	Product	in.	hr/F	4 day	4 week	Rating, mo
Alloy 2090			Plate	0.5	T81	ED,ED[c]	P,P	N (24)
			Extrusion	0.4	T83	ED,ED	P,P	N (24)
2.2	2.5	0.12	Plate	0.25	24/325	ED	P	N (48)
2.2	3.0	0.12	Plate	0.25	24/325	ED	P	N (48)
2.5	2.5	0.12	Plate	0.25	24/325	ED	P	N (48)
2.5	3.0	0.12	Plate	0.25	24/325	ED	P	N (48)
2.2	2.5	0.12	Plate	1	24/325	EA	P	EA (48)
2.2	3.0	0.12	Plate	1	24/325	EA	P	EA (48)
2.5	2.5	0.12	Plate	1	24/325	EA	P	EA (48)
2.5	3.0	0.12	Plate	1	24/325	EC	P	EA (48)

Note: The 0.5 inch plate and the extrusion were produced as part of the Navy sponsored cooperative test program. The 0.25 inch and 1 inch plates were cast as small ingots and rolled at the Alcoa Technical Center as part of the 2090 development program.

(a) Total immersion in 4N, NaCl + 0.5N, KNO_3 + 0.1N, HNO_3 solution for 48 hours – ASTM Method G34-86.
(b) Exposure to acetic acid acidified salt spray, ASTM Method G85, Annex 2.
(c) Ratings according to ASTM Method G34-72: P = pitting, and E = exfoliation; severity is denoted by the letter A, B, C, or D in increasing severity.

TABLE 2.0313. CORROSION TEST COMPARISON, 2090 PLATE (38)

Alloy	2090					
Temper	T83					
Form	Plate					
		EXCO[a],	MASTMAASIS[b]			Point Judith
Condition	Plane	4 day	Wet	Dry	Asset	Rating, mo
As-Received	T/2	ED[d]	P[c]			N (24)
(T83)	T/10	ED[d]	P	P	P	N (24)
As-Quenched	T/2	EB	EA	ED	EC	ED (24)
(212 F Water)	T/10	EC	EA	ED	EC	ED (24)
As-Quenched	T/2	EA	EA	EB	EC	EC (24)
(68 F Water)	T/10	EA	EA	EC	EC	ED (24)

(a) Total immersion in 4N, NaCl + 0.5N, KNO_3 + 0.1N, HNO_3 solution for 48 hours – ASTM Method G34-86.
(b) Exposure to acetic acid acidified salt spray, ASTM Method G85, Annex 2.
(c) Ratings according to ASTM Method G34-72: P = pitting and E = exfoliation; severity is denoted by the letter A, B, C, or D in increasing severity.
(d) Specimens removed from test after 2 days.

TABLE 2.0314. ACCELERATED CORROSION TESTS OF 0.5-INCH PLATE OF 2090 (38)

Al
2.7 Cu
2.3 Li
0.12 Zr

2090 Al

Al
2.7 Cu
2.3 Li
0.12 Zr

2090 Al

Alloy		2090							
Temper		T83							
Form		1-inch Plate							
Composition, weight percent		Alternate Immersion[a]				Point Judith, Rhode Island			
		25 ksi		35 ksi		25 ksi		35 ksi	
Li	Cu	F/N[b]	Days	F/N	Days	F/N	Days	F/N	Days
2.5	3.0	0/3	–	3/3	3,3,5	0/3	–	2/3	367,367
2.2	3.0	0/3	–	1/3	9	0/3	–	1/3	966
2.5	2.5	1/3	5	3/3	3,3,3	0/3	–	3/3	367,839 966
2.2	2.5	0/3	–	3/3	3,9,9	0/3	–	0/3	–

(a) ASTM G47 test; ASTM G44 solution.
(b) Number of specimens failed/number exposed.

TABLE 2.0321. STRESS CORROSION OF 2090-T83 PLATE, EFFECT OF COMPOSITION (4)

Alloy	2090						
Temper	T83						
Form	Extrusion						
Test	Alternate Immersion[a]						
Aging Treatment, hr at 325 F	Stress, ksi (L)	25 ksi		35 ksi		45 ksi	
		F/N	Days	F/N	Days	F/N	Days
10	64.4	4/6	10,19,28,28	3/6	9,15,28	6/6	3,3,3,5,5,6
18	72.8	0/6	–	0/6	–	2/6	20,25
24	73.2	0/6	–	0/6	–	1/6	4
36	74.2	0/6	–	0/6	–	1/6	12
Note: All aged conditions survived 30 days at 15 ksi.							

(a) ASTM G47 test method; ASTM G44 solution.

TABLE 2.0322. STRESS CORROSION OF 2090-T83 EXTRUSION, EFFECT OF AGING (4)

Alloy	2090		
Form	Plate		
Times to Failure (days) After NaCl Immersion for 6 Days[a]			
Environment		Alloy 2024	Alloy 2090UA[b]
Lab Air (≈50% R.H.)		>60[c]	0.6 ± 0.1[d]
Lab Air (≈100% R.H.)		5 ± 1	–
CO_2-Free Air (≈100% R.H.)		>60	>60
Times to Failure (days) Under Constant Immersion			
Added Species[e]	Alloy 2024	Alloy 2090UA	Alloy 2090PA[f]
None	>60	>30	>30
LiCl	>60	16.0 ± 3.0[d]	10.7 ± 2.7
Li_2CO_3	5.7 ± 1.5	1.0 ± 0.3	1.70 ± 0.1
Na_2CO_3	>60	>60	>60

(a) Naturally aerated 3.5% NaCl in distilled water; specimens stressed to 35 ksi in the environments listed.
(b) UA = underaged.
(c) "> X" = test ended after X days, with no failures.
(d) Mean ± standard deviation.
(e) All environments have aerated 3.5 w/o NaCl as their base, with 0.1 M of the listed species added. The exception is LiCl, where 0.2 M LiCl was added to 2.6 w/o NaCl, in an effort to keep Cl^- and Li^+ concentrations consistent with Li_2CO_3. All initial pH = 10. Chemicals were all reagent grade.
(f) PA = peak aged.

TABLE 2.0323. TIME TO FAILURE FOR 2090 1.5-INCH PLATE IN VARIOUS ENVIRONMENTS (36)

Al	
2.7	Cu
2.3	Li
0.12	Zr

2090 Al

Alloy	2090			
Environment	3.5% NaCl, Alternate Immersion[a]			
Specimen-Heat Treat	Stress Method	Induced Stress	Hours in Solution	Condition
2090-T3	U-bend[b]	36.2	428	Severe exfoliation and pitting; no IG[c]
2090-T3	U-bend	33.6	240	Exfoliation, no IG nor SCC
2090-T3	U-bend	36.2	240	Exfoliation, no IG
2090-T8	U-bend	40.6	91	Heavily pitted, heavy IG
2090-T8	U-bend	43.5	48	24 hrs crack 0.012-in. deep 48 hrs crack 0.02-in. deep Also heavily pitted
2090-T8	U-bend	45.7	18	IG, SCC[d], delamination, pitting
2090-T8	U-bend	43.5	10	Mainly pitting, no IG nor SCC

(a) ASTM G47.
(b) U-bend = U-bend specimen in the longitudinal direction.
(c) IG = intergranular cracking.
(d) SCC = stress corrosion cracking (cracking initiated at the stressed edge).

TABLE 2.0324. STRESS CORROSION DATA (TIME TO FAILURE) FOR 2090 SHEET (37)

Alloy	2090	
Environment	3.5% NaCl, Alternate Immersion[a]	
Crevice Corrosion Test		
Specimen-Heat Treat	Hours in Solution	Condition
2090-T8	336	In O_2-depleted area, severe pitting similar to 2024, no delamination
2024-T3	336	In O_2-depleted area, severe pitting

(a) ASTM G47.

TABLE 2.0325. CREVICE CORROSION OF 2090 SHEET (37)

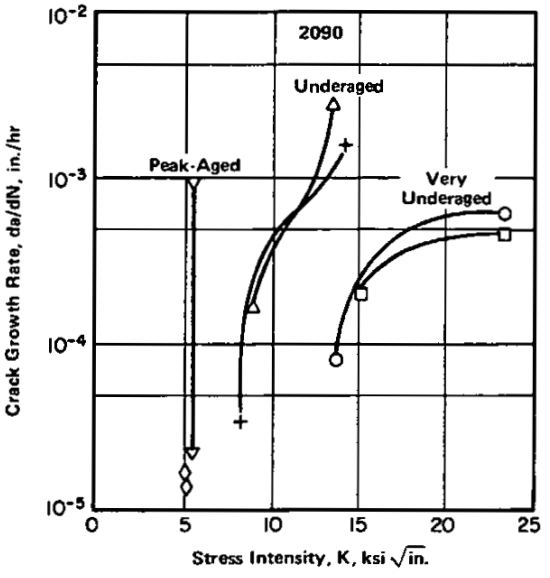

FIGURE 2.0326. STRESS CORROSION CRACK GROWTH RATE FOR 2090 T-X EXTRUSIONS IN 3.5% NaCl (10)

Al
2.7 Cu
2.3 Li
0.12 Zr

2090 Al

Alloy	2090								
Temper	T81								
Form	Plate								
Test Type	1/8-inch Diameter Tension								
Thickness, in.	0.5	1.5							
Direction	T	ST							
Environment	(a)	(a)			(b)			(c)	
Exposure Stress, ksi	60	20	25	35	15	25	35	25	35
Exposure Time, days	30	30	30	30	120	120	120	150	150
No. Failed/No. Tests	0/5	0/5	4/5	5/5	0/5	4/5	5/5	0/5	1/5
Failure Time Range, days	–	–	1–10	2–9	–	13–19	13	–	105

(a) 3.5% NaCl alternate immersion per ASTM G44.
(b) Seacoast, Point Judith, RI.
(c) Mild industrial inland, New Kingsington, PA.

TABLE 2.0327. STRESS CORROSION RESULTS FOR 2090-T81 PLATE IN VARIOUS ENVIRONMENTS (49)

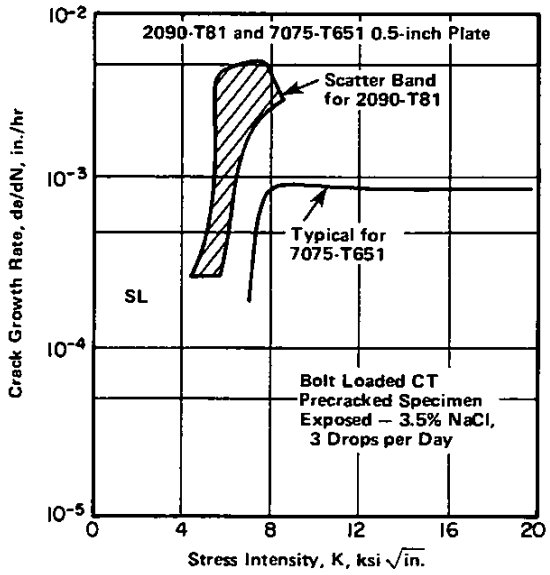

FIGURE 2.0328. STRESS CORROSION CRACK GROWTH RATES IN 3.5% NaCl FOR 2090-T81 AND 7075-T651 PLATE TESTED IN THE SL DIRECTION (49)

Alloy	2090				
Form	Plate				
Temper	Condition	F_{ty}, ksi	F_{tu}, ksi	Elongation, percent	Percent Loss in Elongation
T6	Charged	70.9	71.8	6.3	36
	Uncharged	73.2	79.8	9.8	–
Overaged	Charged	49.6	57.7	3.9	65
	Uncharged	56.6	66.0	11	–
Tensile specimens chemically polished and cathodically charged in 0.1N HCl, pH = 1 or 0.5N H_2SO_4 at -2000 mV.					

TABLE 2.0341. EFFECT OF HYDROGEN CHARGING ON THE MECHANICAL PROPERTIES OF 2090 PLATE (39)

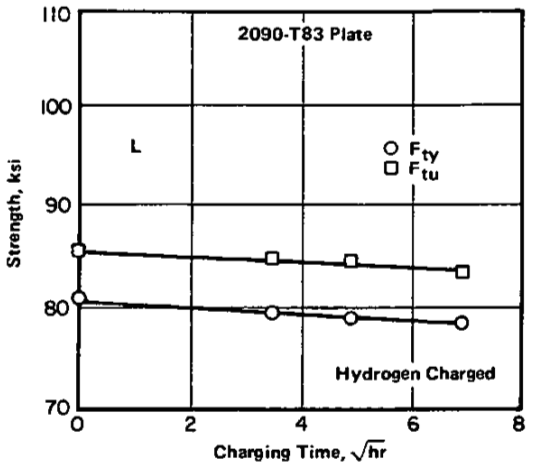

FIGURE 2.0342. EFFECT OF HYDROGEN CHARGING ON THE STRENGTH OF 2090-T83 0.5-INCH PLATE (40)

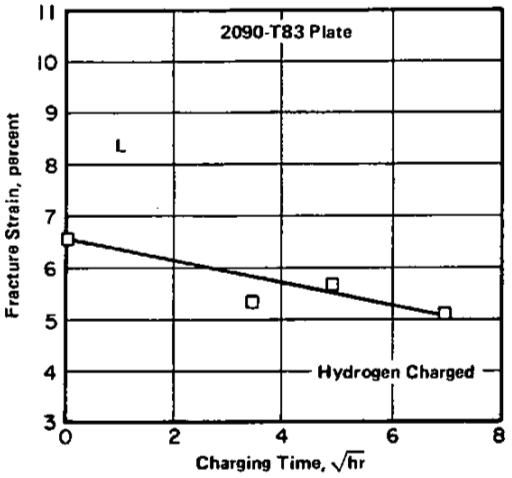

	Al
2.7	Cu
2.3	Li
0.12	Zr

2090 Al

FIGURE 2.0343. EFFECT OF HYDROGEN CHARGING ON THE FRACTURE STRAIN OF 2090-T83 0.5-INCH PLATE (40)

Alloy	2090					
				Minimums		Elongation,
Condition	Form	Thickness, in.	Direction	F_{tu}, ksi	F_{ty}, ksi	percent in 2 in.
0	Sheet	0.032–0.249	–	31.0 max	28.0 max	11
T3	Sheet	0.032–0.249	–	46.0	31.0	6
T31	Sheet	0.032–0.249	–	42.0	28.0	11
				55.0 max	42.0 max	–
T81	Plate	0.500–1.5	L	75.0	70.0	4
			T	75.0	68.0	3
T83	Sheet	0.032–0.125	L	77.0	70.0	3
			T	73.0	66.0	5
		0.126–0.249	L	75.0	70.0	4
			T	73.0	66.0	5
T84	Sheet	0.032–0.249	L	72.0	66.0	3
			T	69.0	60.0	5
T86	Extrusion	Up to 0.124	L	77.0	71.0	4
		0.125–0.249	L	77.0	72.0	4
		0.250–0.499	L	78.0	72.0	5
			T	75.0	70.0	3

TABLE 3.011. ALUMINUM ASSOCIATION REGISTERED TEMPERS (2)

	Al
2.7	Cu
2.3	Li
0.12	Zr

2090 Al

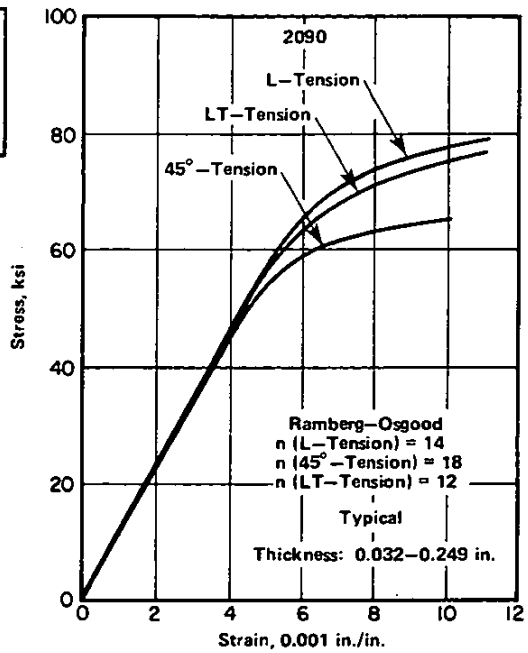

FIGURE 3.0211. STRESS STRAIN CURVE FOR 2090-T83 SHEET (1)

Alloy	2090				
Form	0.5 inch Plate				
Temper	T83				
Source	(5)		(8)		
Orientation	L	T	L	T	45 Degree
F_{tu}, ksi	85	85	85	84	75
F_{ty}, ksi	75	80	80	80	67
Elongation, percent	7.6	6.2	9.3	5.4	11

TABLE 3.0212. TENSILE PROPERTIES OF 2090-T83 PLATE FROM TWO SOURCES (5,8)

Alloy	2090				
Form	Thickness or Shape	Temper	F_{tu}, ksi	F_{ty}, ksi	Elongation, percent
Sheet	0.12 in.	T6	78.3	70.3	5
		Underaged	66.0	55.1	7
Plate	0.79 in.	T6	76.9	70.3	6
Extrusion	L-Shape	T6	81.9	74.7	6
	1 x 5 x 6 in.	Underaged	68.2	55.1	8
Hand Forging	3 x 6 in.	T6	74.7	60.2	5
Die Forging	Complex	T6	68.2–79.8	50.0–70.3	2–8

TABLE 3.0213. TENSILE PROPERTIES OF VARIOUS 2090 PRODUCT FORMS IN THE -T6 AND UNDERAGED TEMPERS (10)

Alloy		2090		
Temper		T83		
Form		Extrusion		
Lot		F_{tu}, ksi	F_{ty}, ksi	Elongation, percent
1	Rear[a]	85.6	79.7	6.0
	Front	82.7	78.0	6.5
2	Rear	88.3	82.2	5.5
	Front	87.0	81.3	5.5

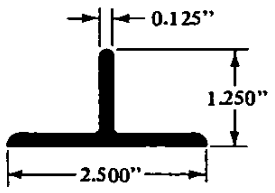

(a) Front and rear denote initial and final sections of extrusion length from a billet.

TABLE 3.0214. TENSILE PROPERTIES OF 2090-T83 EXTRUSION (9)

Al
2.7 Cu
2.3 Li
0.12 Zr

2090 Al

Alloy	2090			
Form	Sheet			
Temper	T3			
Thickness/ Lot	Test Direction	F_{tu}, ksi	F_{ty}, ksi	Elongation, percent in 2 in.
0.090 in.				
A	Longitudinal	39.9	25.3	18.8
	Transverse	44.1	26.4	19.0
B	Longitudinal	46.9	31.2	18.8
	Transverse	46.9	29.5	19.3
0.125 in.				
C	Longitudinal	48.4	32.8	11.5
	Transverse	48.4	30.6	16.5

TABLE 3.0215. TENSILE PROPERTIES OF 2090-T3 SHEET (35)

Alloy	2090						
Form	Sheet						
Temper		F_{tu}, ksi		F_{ty}, ksi		Elongation, percent in 2 in.	
T83	Orientation	T	L	T	L	T	L
	0.125 in.						
	Process 2[a]	80.3	84.3	73.8	81.0	6.7	4.1
	Process 1	79.1	82.2	71.3	75.9	6.6	4.8
	Lot Average	79.5	82.6	72.6	77.4	6.3	4.5
	0.063 in.						
	Lot Average	78.2	80.5	71.3	73.5	6.1	5.0
T31	Lot A	63.9	63.5	49.8	54.2	12.0	5.9
	Lot B	64.8	63.2	51.8	54.5	10.1	5.8
	Lot C	67.2	68.4	53.3	60.8	10.8	5.0

(a) Processes 1 and 2 not specified in (35).

TABLE 3.0216. TENSILE PROPERTIES OF 2090-T31 AND -T83 SHEET (35)

Alloy	2090			
Temper	T83			
Form	Sheet			
		Tensile Strength		Elongation,
Thickness, in.	Orientation	F_{tu}, ksi	F_{ty}, ksi	percent
0.090	L	83.9	77.2	5.5
	T	80.5	74.3	7.5
0.144	L	83.1	76.6	6.0
	T	79.3	72.8	9.0
0.190	L	82.1	76.2	6.5
	T	78.7	72.4	9.0

TABLE 3.0217. TENSILE PROPERTIES OF 2090-T83 SHEET (9)

	Al
2.7	Cu
2.3	Li
0.12	Zr

2090 Al

Alloy	2090			
Form	Sheet (Superplastically Formed)(a)			
Temper	T6			
Area(b)	Thickness, in.	F_{ty}, ksi	F_{tu}, ksi	Elongation, percent
A	0.028	48.1	63.5	8.9
B	0.028	49.2	65.1	8.5
C	0.032	46.2	62.6	9.7
D	0.042	46.0	58.9	12.9
E	0.025	46.3	62.1	11.2
F	0.027	44.8	61.7	12.5
G	0.034	43.2	58.6	8.5
Flange	0.073	46.5	65.5	7.8
Unformed Sheet	0.074	44.5	60.1	8.9

(a) For illustration of component, see Table 1.063.
(b) Areas on drawn sidewall: A, E, F, G; areas on bottom: B, C, and D.

TABLE 3.0218. TENSILE PROPERTIES OF SUPERPLASTICALLY FORMED 2090-T6 SHEET (6)

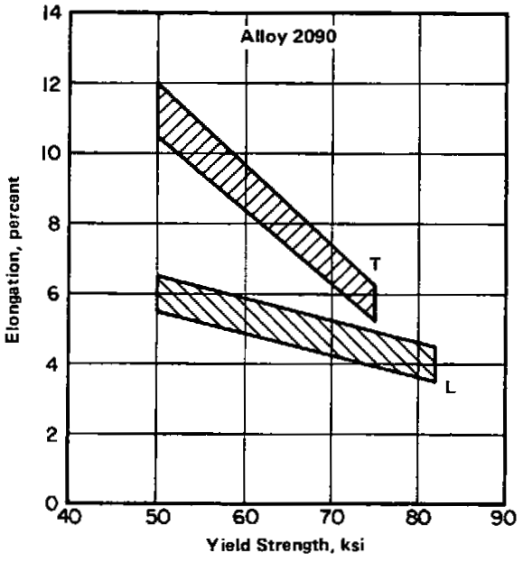

FIGURE 3.0219. STRENGTH-DUCTILITY RELATIONSHIPS FOR 0.090-INCH 2090 SHEET IN VARIOUS TEMPERS (35)

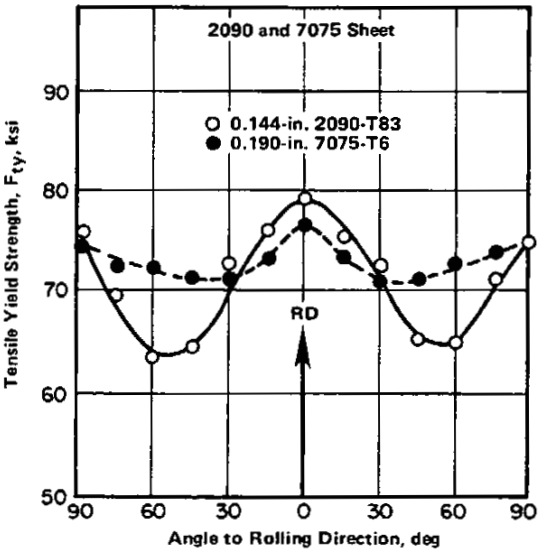

FIGURE 3.02110. YIELD STRENGTH AS A FUNCTION OF ORIENTATION TO THE ROLLING DIRECTION FOR 2090-T83 AND 7075-T6 SHEET (49)

	Al
2.7	Cu
2.3	Li
0.12	Zr

2090 Al

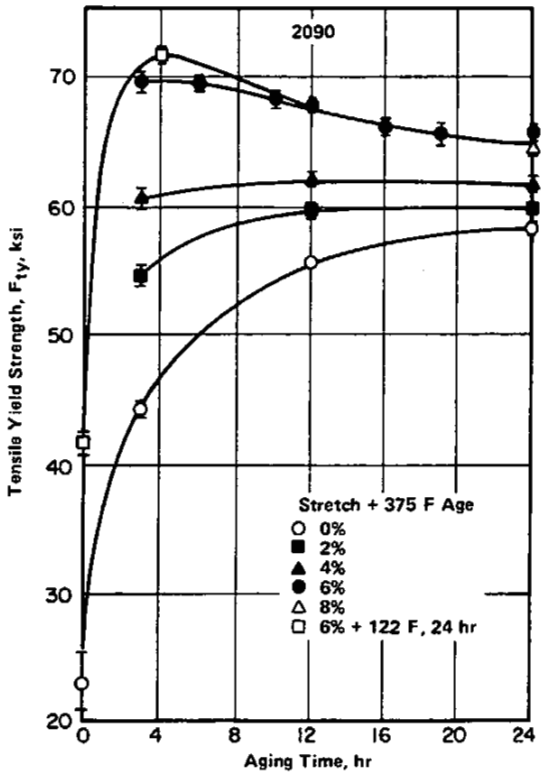

FIGURE 3.02111. YIELD STRENGTH AS A FUNCTION OF STRETCHING AND AGING AT 375 F (11)

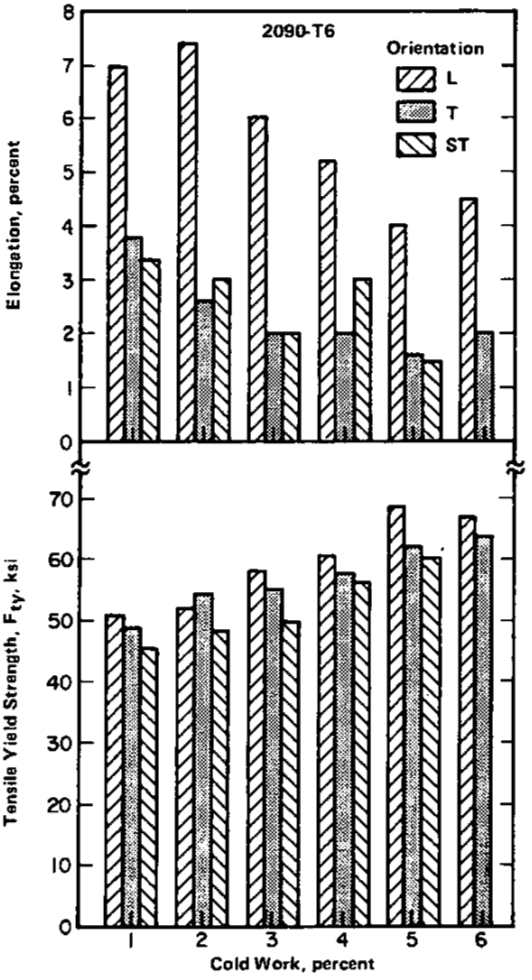

FIGURE 3.02112. YIELD STRENGTH AND ELONGATION AS A FUNCTION OF COLD WORK BEFORE AGING IN 2090-T6 HAND FORGINGS (11)

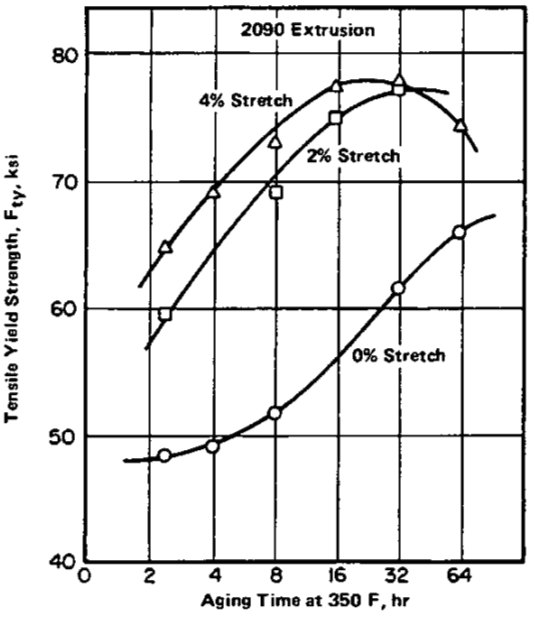

FIGURE 3.02113. TRANSVERSE YIELD STRENGTH AS A FUNCTION OF COLD WORK BEFORE AGING IN 2090 EXTRUSIONS (11)

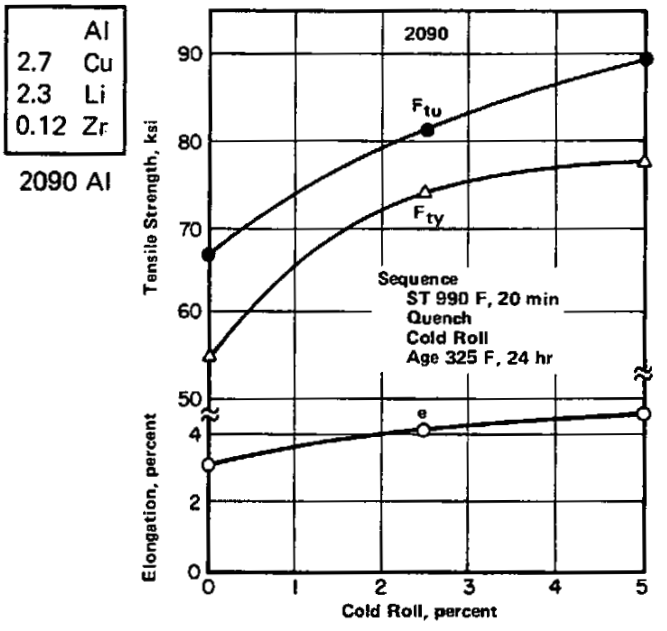

FIGURE 3.02114. TENSILE PROPERTIES AS A FUNCTION OF COLD WORK (ROLLING) BEFORE AGING IN 2090 SHEET (7)

Alloy	2090		
Form	Plate and Extrusion		
Temper	T8		
Orientation	F_{tu}, ksi	F_{ty}, ksi	Elongation, percent
As-Received			
Plate			
L	84.2	78.0	6.6
LT	82.1	76.1	8.5
Extrusion			
LX	82.3	78.0	6
TX	70.6	66.3	11
After 1000 hr at 150 F			
Plate			
L	88.8	82.6	2.5
LT	88.6	80.6	6
Extrusion			
LX	86.1	82.9	1.5
TX	80.6	75.9	5

TABLE 3.02115. EFFECT OF EXPOSURE AT 150 F ON THE TENSILE PROPERTIES OF 2090 PLATE AND EXTRUSION (SEE ALSO TABLE 3.02727) (33)

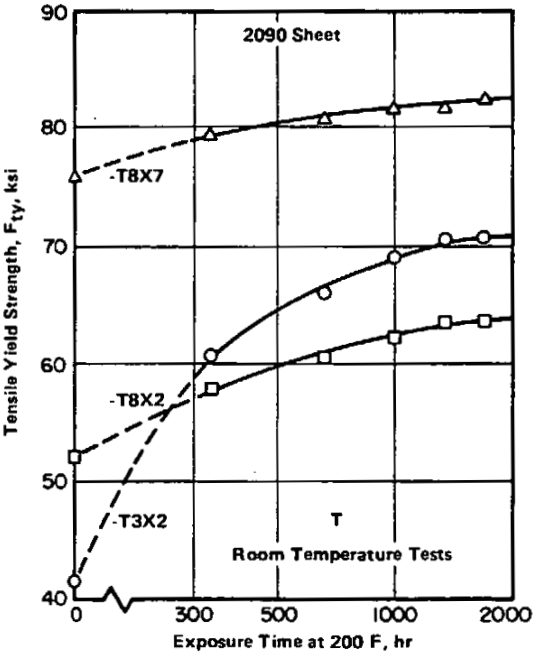

FIGURE 3.02116. EFFECT OF EXPOSURE AT 200 F ON THE TENSILE PROPERTIES OF 2090 SHEET (SEE ALSO 3.02727) (34)

Alloy	2090	
Temper	T83	
Form	Sheet	
Thickness, in.	Orientation	Compressive Yield Stress, F_{cy}, ksi
0.090	L	77
	T	81.4
0.144	L	73.9
	T	78.7
0.190	L	74.5
	T	78.2

TABLE 3.0221. COMPRESSIVE YIELD STRENGTH OF 2090-T83 SHEET (9)

Alloy	2090			
Product Form		Compressive Yield Strength, F_{cy}, ksi		
Sheet Thickness, in.	Temper	L	45 Degree	LT
0.032–0.125	T83	67	58	71
0.125–0.249	T83	63	60	71

TABLE 3.0222. PROPOSED COMPRESSIVE YIELD DESIGN ALLOWABLES FOR 2090-T83 SHEET (1)

Al	
2.7	Cu
2.3	Li
0.12	Zr

2090 Al

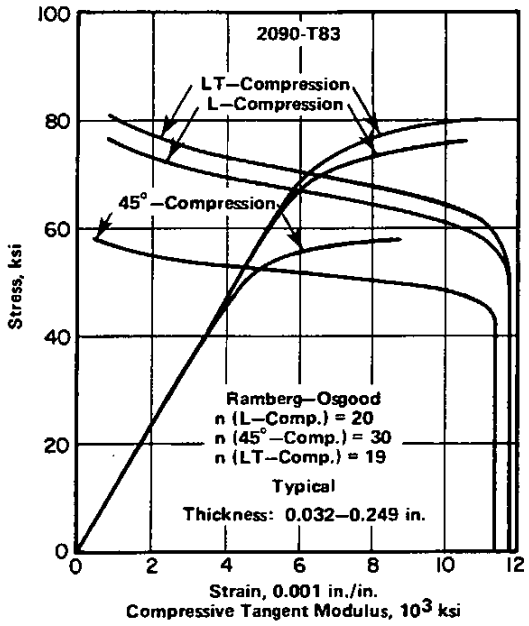

FIGURE 3.0223. COMPRESSIVE STRESS-STRAIN AND TANGENT MODULUS CURVES FOR 2090-T83 SHEET (1)

Alloy	2090			
Temper	Various			
Form	Plate			
Orientation			L-T	L
Cold Work (Stretch), percent	Aging Temperature, F	Aging Time, hr	Charpy Values, in.-lb/in.^{2}	F_{ty}, ksi
0	347	36	135	60.3
3	297	24	520	59.6
7	250	60	600	61.8

TABLE 3.0231. CHARPY V RESULTS FOR 2090 PLATE COLD WORKED VARIOUS AMOUNTS AND AGED TO EQUIVALENT STRENGTH (23)

	Al
2.7	Cu
2.3	Li
0.12	Zr

2090 Al

Alloy	2090	
Temper	T83	
Form	Sheet	
Thickness, in.	Orientation	Ultimate Shear Strength, F_{su}, ksi
0.090	L	41.6
	T	43.9
0.144	L	41.1
	T	44.3
0.190	L	41.9
	T	44.2

TABLE 3.0251. SHEAR STRENGTH OF 2090-T83 SHEET (9)

Alloy	2090			
Temper	T83			
Form	Sheet			
		Bearing		
		F_{bu}, ksi		F_{by}, ksi	
Thickness, in.	Orientation	e/D = 1.5	e/D = 2.0	e/D = 1.5	e/D = 2.0
0.090	L	116.3	145.8	98.6	113
	T	115.3	148.8	98.1	121.4
0.144	L	110.7	146.3	99.2	117.1
	T	114.1	141.2	99.7	119.2
0.190	L	112.7	147.3	99.2	111.7
	T	115.6	144.7	101	117.7

TABLE 3.0261. BEARING PROPERTIES OF 2090-T83 SHEET (9)

Alloy		2090	
Dry Pin Bearing Values		F_{bry}, ksi	
Product Form	Temper	e/D = 1.5	e/D = 2.0
Sheet 0.032–0.249 in.	T83	100	126

TABLE 3.0262. PROPOSED DESIGN ALLOWABLE BEARING STRENGTHS FOR 2090-T83 SHEET (1)

Alloy	2090									
Temper	T83									
Form	0.053-inch Sheet									
Test Method	R Curves by ASTM E561 With Analysis by ASTM B646									
Specimen Type	M(T) W = 16 in. 4 in. Crack		M(T) W = 6 in. 2 in. Crack		M(T) W = 6 in. 1.5 in. Crack		M(T) W = 4 in. 1.5 in. Crack		C(T) W = 14 in.	
Orientation	LT	TL	LT	TL	LT	TL	LT	TL	LT	TL
No. of Tests	4	3	1	1	1	1	2	2	1	1
K_c Avg., ksi $\sqrt{in.}$	49	32	46	27	–	–	38	32	46	43
K_c Spread	42–59	30–35	–	–	–	–	36–40	23–41	–	–
K_{app}, ksi $\sqrt{in.}$(a)	43	31	27	30	38	37	36	27	–	–
K_{app} Spread	38–50	28–33	–	–	–	–	37–37	23–32	–	–

(a) Based on original crack length.

TABLE 3.02721. FRACTURE TOUGHNESS VALUES FOR 2090 SHEET (49, TABLE A6)

Alloy	2090			
Form	Sheet			
Temper	T31			
Gauge	0.090 inch			
Orientation	L-T		T-L	
Lot No.	K_c[a], ksi $\sqrt{in.}$	K_{app}, ksi $\sqrt{in.}$	K_c, ksi $\sqrt{in.}$	K_{app}, ksi $\sqrt{in.}$
A[b]	86.1	65.1	92.7	69.7
	106.3	77.8	–	–
(c)	104.8	77.6	–	–
(d)	97.1	61.9	–	–
(e)	109.1	69.8	–	–
B	89.4	66.9	94.6	69.3
	91.3	69.1	–	–
C	83.3	69.1	94.7	71.6
	88.0	64.2	–	–

(a) See 3.0272 for a discussion of test methods.
(b) Determined on 16 inch wide panel to ASTM E561 and B646, tested at full thickness.
(c) Machined to 0.049 inch at mid thickness.
(d) Machined to 0.039 inch from one side.
(e) Machined to 0.036 inch from one side.

TABLE 3.02722. FRACTURE TOUGHNESS OF DAMAGE TOLERANT 2090 SHEET (35)

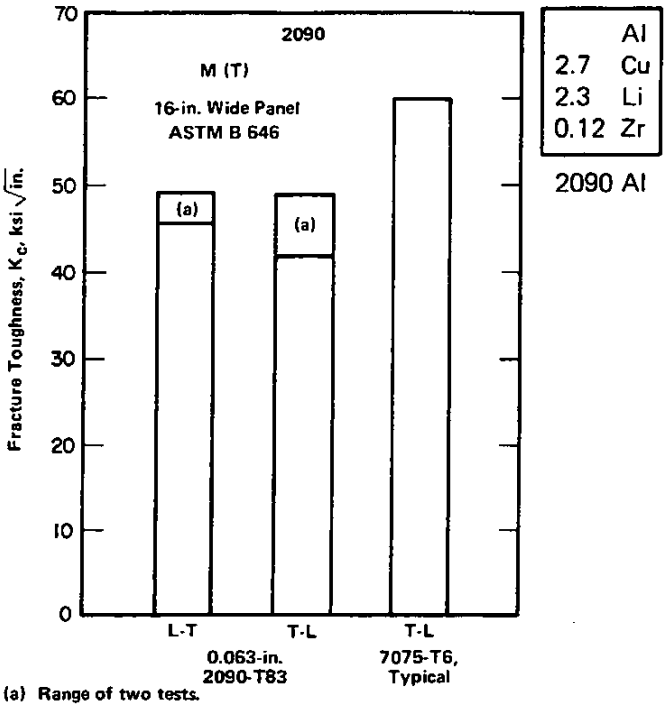

(a) Range of two tests.

FIGURE 3.02723. FRACTURE TOUGHNESS OF 2090-T83 SHEET (22)

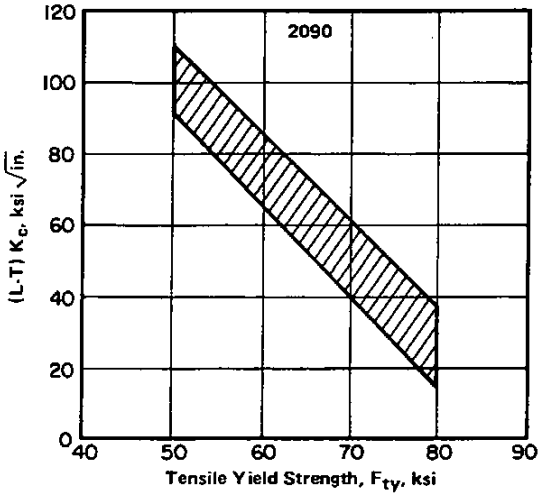

FIGURE 3.02724. FRACTURE TOUGHNESS OF PRODUCTION 2090 SHEET AS A FUNCTION OF STRENGTH LEVEL (35)

Alloy	2090	
Form	Sheet	
Temper	T8	
Orientation L-T	ksi $\sqrt{in.}$	
Thickness, in.	K_c[a]	K_{app}[a]
0.063	44.1	40.0
0.063	53.0	
0.063	38.0	
0.125 (Process 1)	38.3	35.9
0.125 (Process 2)	35.9	33.4

(a) See 3.0272 for discussion of test methods.

TABLE 3.02725. FRACTURE TOUGHNESS OF 2090 PEAK-AGED SHEET (35)

	Al
2.7	Cu
2.3	Li
0.12	Zr

2090 Al

Alloy	2090		
Thickness	0.5 inch		
Orientation	L-T		
Form	Thickness or Section, in.	Temper	Toughness, K_{Ic} or K_Q, ksi $\sqrt{in.}$(a)
Sheet	0.12	T6	50
Sheet	0.12	Underaged	100
Plate	0.8	T6	31.8
Extrusion	L Shape, 1 x 5 x 6	T6	18.2
Extrusion	L Shape, 1 x 5 x 6	Underaged	31.8

(a) Determined by ASTM E399.

TABLE 3.02726. FRACTURE TOUGHNESS OF VARIOUS 2090 FORMS (10)

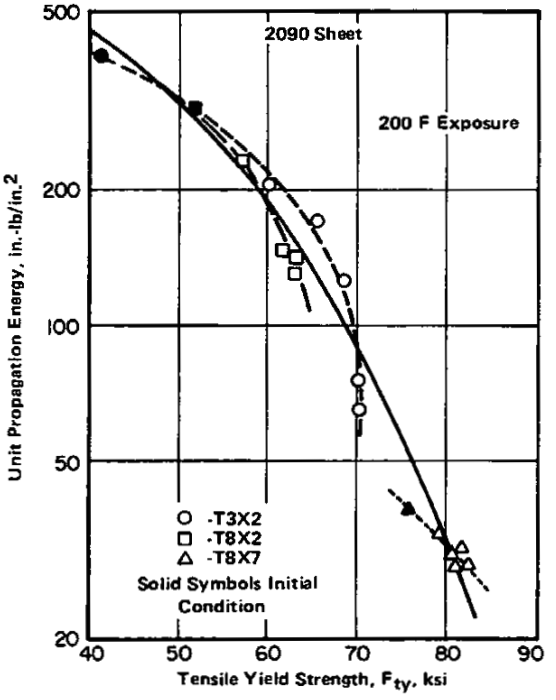

FIGURE 3.02727. EFFECT OF EXPOSURE FOR 0 TO 6 WEEKS AT 200 F ON THE UNIT PROPAGATION ENERGY IN A KAHN TEST FOR 2090 SHEET (34)

Alloy	2090							
Temper	T81						T86	
Form	0.5 inch Plate			1.5 inch Plate			Extrusion(a)	
Orientation	L-T	T-L	T-L + 45	T-L	S-L	S-T	L-T	T-L
K_{Ic} Avg., ksi $\sqrt{in.}$(b)	29	29	35	25	12	9	24	19
s, ksi(c)	2.4	4.0	–	2.8	–	1.4	2.7	2.8
Spread	26–31	26–31	–	23–27	7–17	8–10	19–29	14–22
No. of Tests	9	30	(d)	17	2	5	24	26

(a) T shaped extrusion with 0.75 inch thick test area.
(b) $P_{max}/PQ < 1.2$ but crack straightness requirement not always met.
(c) Sample standard deviation.
(d) Not given.

TABLE 3.02728. PLANE-STRAIN FRACTURE TOUGHNESS FOR PLATE AND EXTRUSIONS FROM A COOPERATIVE TESTING PROGRAM (49, TABLES 21, B5 AND B6)

Al
2.7 Cu
2.3 Li
0.12 Zr
2090 Al

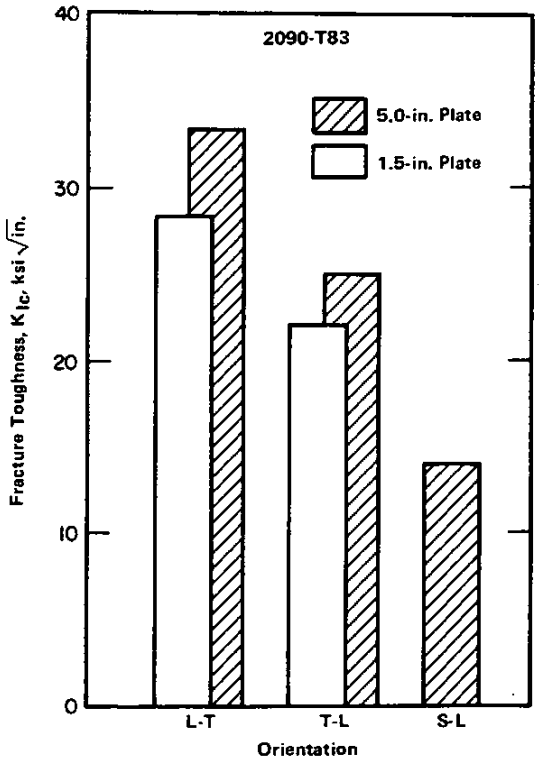

FIGURE 3.02729. PLANE-STRAIN FRACTURE TOUGHNESS OF 2090-T83 PLATE FOR SEVERAL CRACK ORIENTATIONS (22)

Alloy	2090
Form	Plate
Thickness	0.5 inch
Temper	T83
Orientation	Toughness, K_{Ic}, ksi $\sqrt{in.}$
L-T	31.8
T-L	21.8
L + 45/T + 45	25.5

TABLE 3.027210. PLANE-STRAIN FRACTURE TOUGHNESS OF 0.5-INCH 2090-T83 PLATE (8)

Alloy	2090
Form	Plate and Extrusion
Temper	T8
Orientation	Fracture Toughness, K_Q, ksi$\sqrt{in.}$
As-Received Plate (0.5 in.)	
T-L	29.7
L-T	30.2
Extrusion (0.125-in., T-Shape)	
T-L	32
After 1000 hr at 150 F	
Plate (0.5 in.)	
T-L	12.5
L-T	13.7
Extrusion (0.125-in., T-Shape)	
T-L	11.1

TABLE 3.027211. EFFECT OF EXPOSURE AT 150 F ON THE FRACTURE TOUGHNESS OF 2090 PLATE AND EXTRUSION (SEE TABLE 3.02115 FOR TENSILE PROPERTIES) (33)

Al
2.7 Cu
2.3 Li
0.12 Zr

2090 Al

Alloy	2090			
Form	Sheet			
Temper	T83			
Temperature, F	F_{ty}, ksi	F_{tu}, ksi	Elongation, percent	Modulus, ksi x 10^3
70	70.7	76.6	12.0	11.19
	70.6	76.4	12.1	10.27
-323	80.0	92.4	10.5	–
	79.8	93.2	11.1	11.15

TABLE 3.0311. TENSILE PROPERTIES OF 2090-T83 SHEET AT ROOM AND CRYOGENIC TEMPERATURES (16)

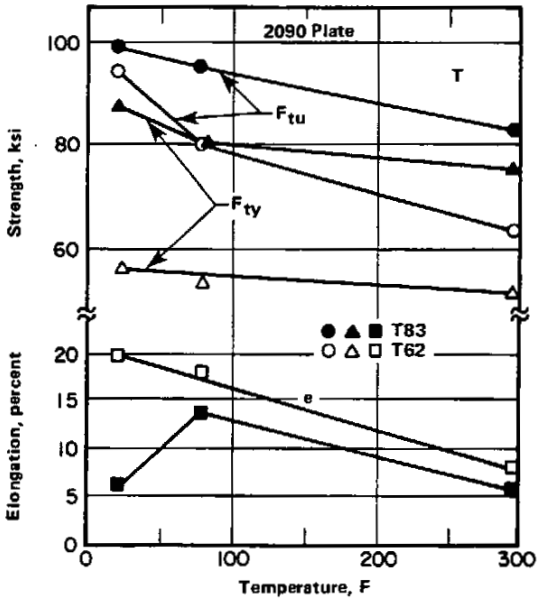

FIGURE 3.0312. TENSILE PROPERTIES OF 0.25-INCH 2090-T62 AND -T83 PLATE AS A FUNCTION OF TEMPERATURE (43)

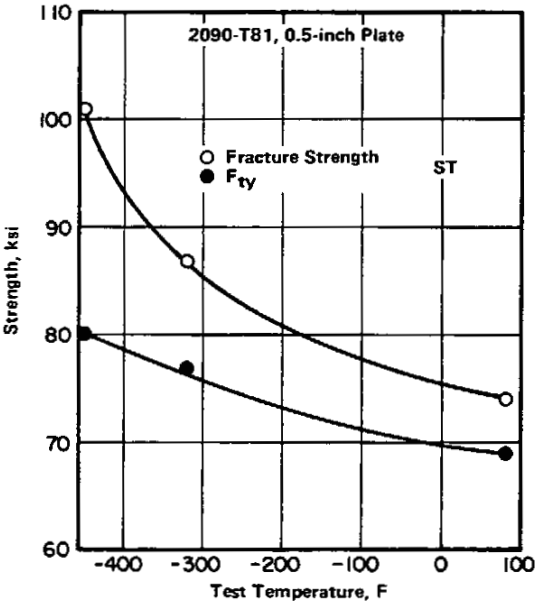

FIGURE 3.0313. EFFECT OF LOW TEST TEMPERATURES ON THE SHORT TRANSVERSE TENSILE STRENGTH OF 2090-T81 PLATE (13)

Alloy	2090				
Form	Sheet				
Temper	T6				
Material	Temp, F	Yield Strength, ksi	Tensile Strength, ksi	Total Elongation, percent	Reduction in Area, percent
2090-T6	63	49	62	5	8
	-320	55	77	15	15

TABLE 3.0314. TENSILE PROPERTIES OF 2090-T6 SHEET (45)

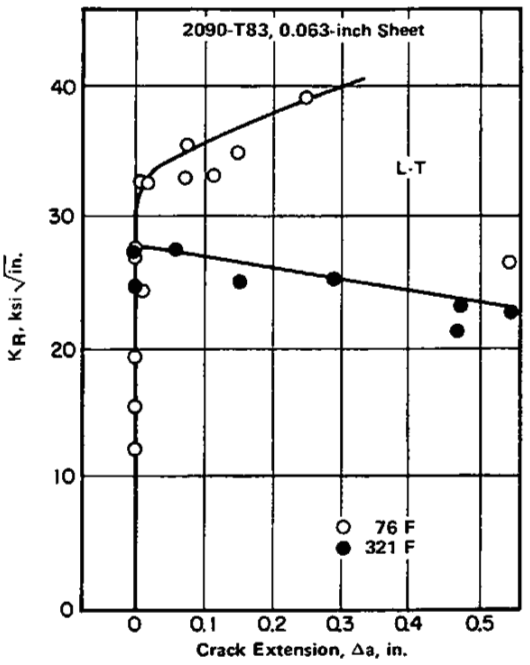

FIGURE 3.03721. R CURVES FOR 2090-T83 SHEET AT AMBIENT AND LIQUID NITROGEN TEMPERATURES (44)

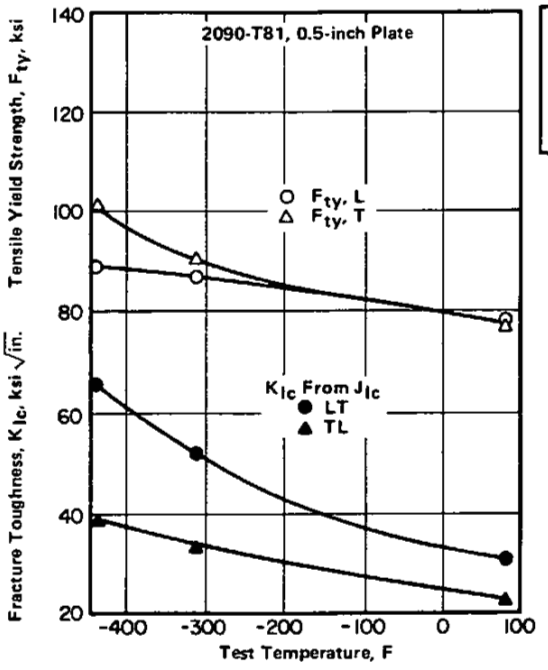

Al
2.7 Cu
2.3 Li
0.12 Zr

2090 Al

FIGURE 3.03722. EFFECT OF LOW TEST TEMPERATURES ON THE TENSILE YIELD STRENGTH AND PLANE-STRAIN FRACTURE TOUGHNESS OF 2090-T81 PLATE (13)

Alloy	2090				
Form	0.5-inch Plate Machined to 0.063-inch at T/4 for Testing				
Temper	T6 and T81				
Material	Test Temp, F	UIE(a), in.-lb/in.^{2}	UPE(b), in.-lb/in.^{2}	Tear Strength, ksi	Tear Yield Ratio
2090-T6	80	144	89	54	1.10
	-320	131	63	57	1.04
2090-T81	80	220	137	65	0.98
	-320	258	218	75	0.98

(a) UIE = unit initiation energy.
(b) UPE = unit propagation energy.

TABLE 3.03723. KAHN TEAR TEST TOUGHNESS (LT) OF 2090-T6 AND -T81 AT AMBIENT AND CRYOGENIC TEMPERATURES (45)

	Al
2.7	Cu
2.3	Li
0.12	Zr

2090 Al

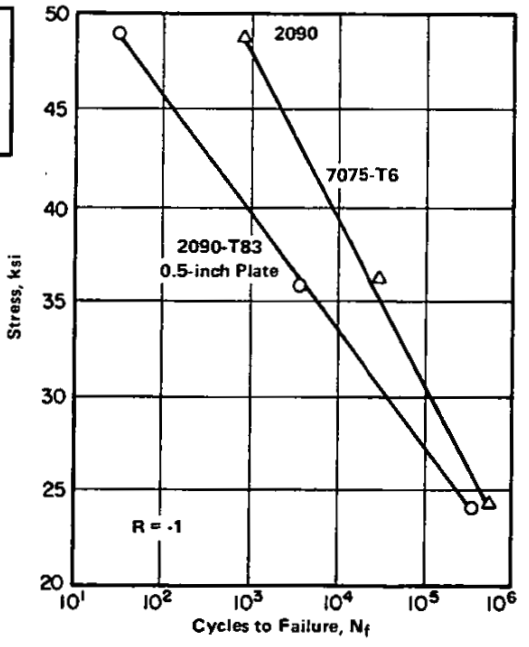

FIGURE 3.0511. FATIGUE LIFE OF 2090-T83 0.5-INCH PLATE IN FULLY REVERSED BENDING (19)

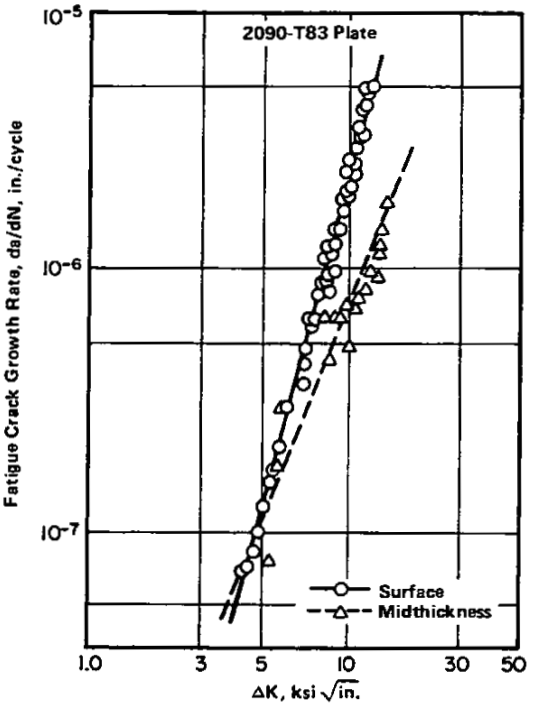

FIGURE 3.0521. FATIGUE CRACK GROWTH RATE CURVES FOR 0.5-INCH 2090-T83 PLATE SHOWING THE EFFECT OF HETEROGENEITY (32)

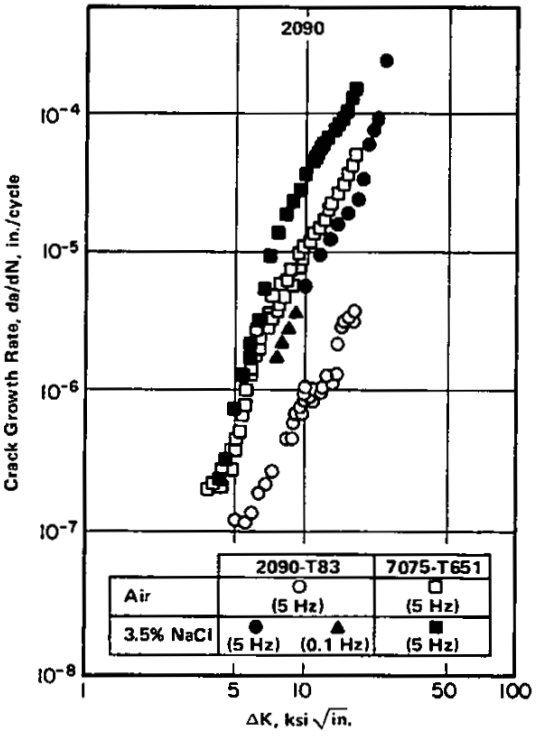

FIGURE 3.0522. FATIGUE CRACK GROWTH RATE FOR 0.5-INCH 2090-T83 PLATE IN AIR AND IN 3.5% NaCl (15)

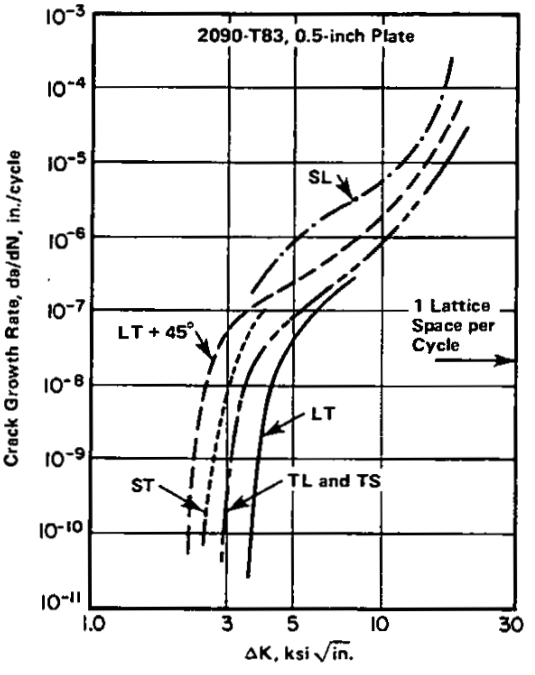

FIGURE 3.0523. FATIGUE CRACK GROWTH RATES FOR 2090-T83 PLATE SHOWING THE EFFECTS OF CRACK ORIENTATION AND K_{th} VALUES (8)

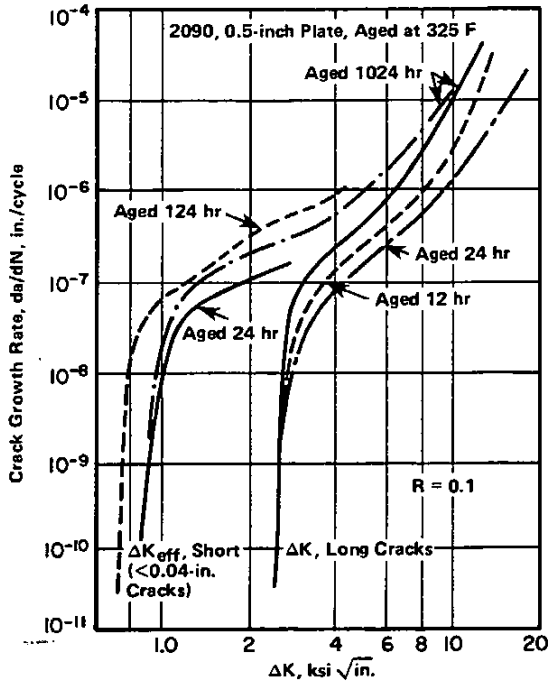

FIGURE 3.0524. FATIGUE CRACK GROWTH RATES FOR LONG AND VERY SHORT CRACKS IN 2090 0.5-INCH PLATE, SHOWING THE EFFECTS OF AGING TIME (8)

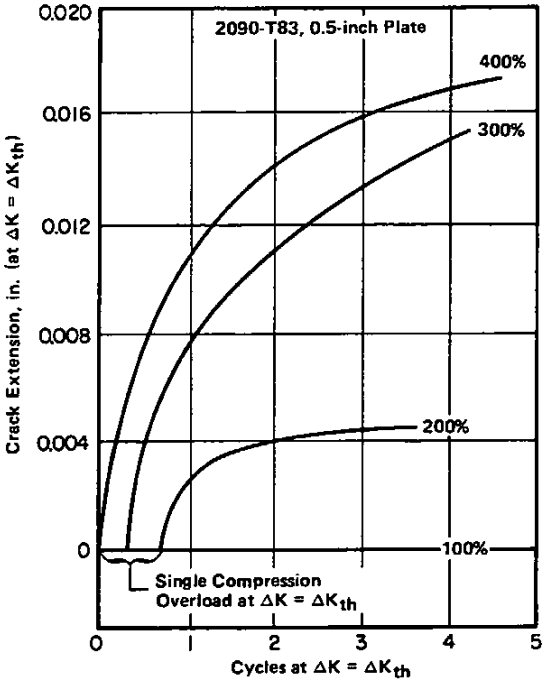

FIGURE 3.0525. CRACK GROWTH AT A CONSTANT VALUE OF $\Delta K = \Delta K_{th}$, FOLLOWING VARIOUS COMPRESSION OVERLOADS (8)

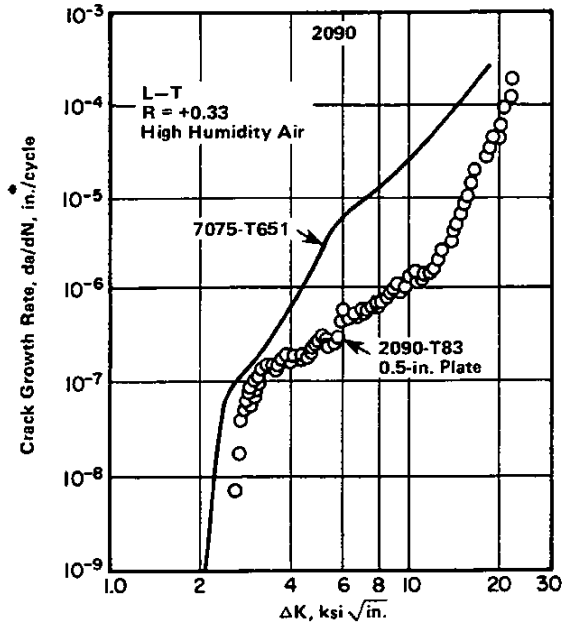

FIGURE 3.0526. FATIGUE CRACK GROWTH RATE OF 2090-T83 0.5-INCH PLATE IN HUMID AIR (5)

Alloy	2090	
Form	Plate	
Temper	T83	
	Modulus	
Orientation	Tension, ksi x 10^3	Compression, ksi x 10^3
L	11.5	12.0
T	11.6	12.1

TABLE 3.061. ELASTIC MODULI OF 2090-T83 PLATE (5)

	Al
2.7	Cu
2.3	Li
0.12	Zr

2090 Al

Alloy	2090							
Form	Sheet							
Temper	T83							
Source	(9)						(1)	
Thickness, in.	0.090		0.144		0.190		0.032–0.249	
Orientation	L	T	L	T	L	T	L & T	T + 45
Tension, 1000 ksi	11.3	11.4	11.3	11.4	11.2	11.3	11.5	11
Compression, 1000 ksi	11.7	11.7	11.6	11.8	11.6	11.8	11.8	11.4

TABLE 3.062. ELASTIC MODULI OF 2090-T83 SHEET FOR SEVERAL TESTING DIRECTIONS (1,9)

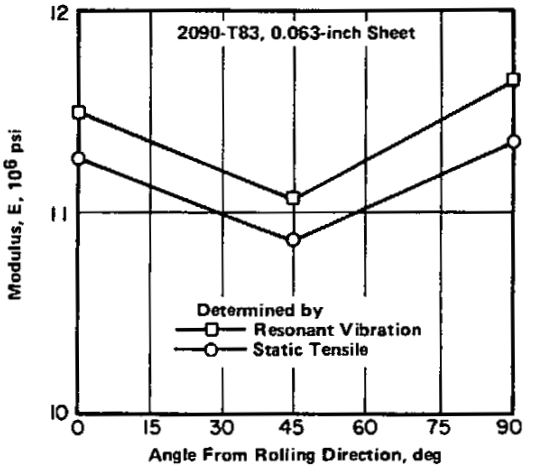

FIGURE 3.063. ANISOTROPY OF YOUNG'S MODULUS IN 2090-T83 SHEET (21)

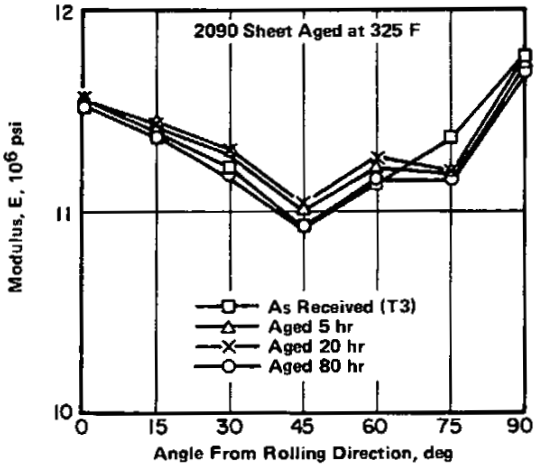

FIGURE 3.064. ANISOTROPY OF YOUNG'S MODULUS IN 2090-T83 SHEET, EFFECT OF AGING AT 325 F (21)

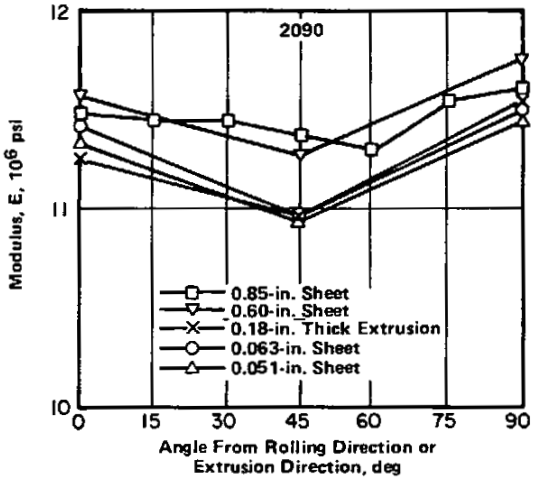

FIGURE 3.065. ANISOTROPY OF YOUNG'S MODULUS IN 2090-T83 SHEET AND EXTRUSION, EFFECT OF THICKNESS (21)

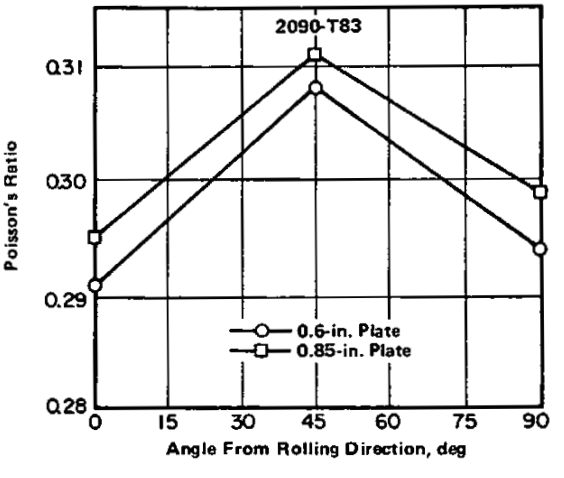

FIGURE 3.066. ANISOTROPY OF POISSON'S RATIO IN 2090-T83 PLATE (21)

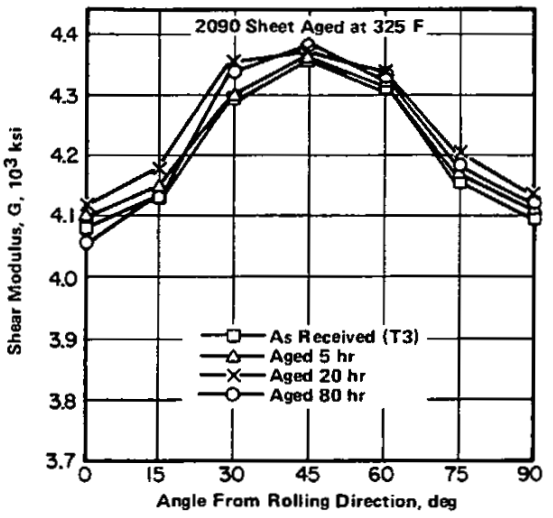

FIGURE 3.067. ANISOTROPY OF SHEAR MODULUS IN 2090 SHEET, EFFECT OF AGING AT 325 F (21)

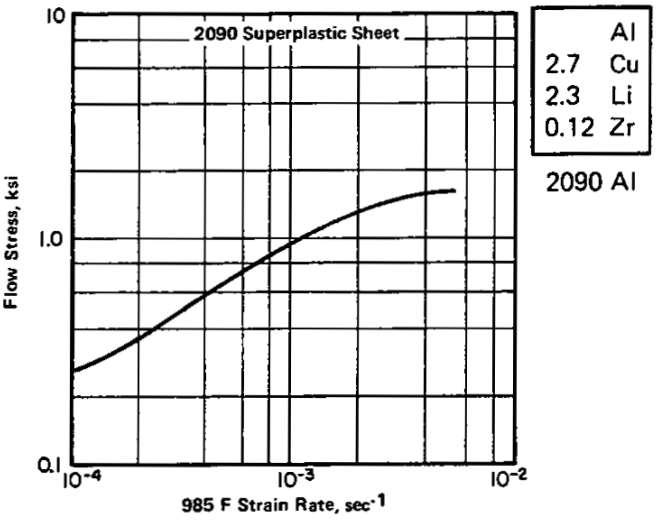

FIGURE 4.011. FLOW STRESS VERSUS STRAIN RATE FOR 2090 SHEET SUPERPLASTICALLY FORMED AT 985 F (46)

Alloy	2090									
Temper	T62[a]		T83							
Form	0.25-in. Sheet		0.25-in. Sheet							
Welding	None	None	Variable Polarity Plasma Arc With EB2319 Filler, Welds Machined Flush							
Post-Weld Treat	None	None	None			T62			30 hr 324 F	
Test Temperature, F	R.T.	-423	R.T.	-320	-423	R.T.	-320	-423	R.T.	-423
F_{tu}, ksi	60	98	40	55	65	60	66	80	47	61
F_{ty}, ksi	49	56	20	29	29	50	55	58	38	38
Elongation, percent	8	22	9	11	10	9	8	8	4	3

(a) 1000 F, WQ + 325 F, 30 hr.

TABLE 4.0312. TENSILE PROPERTIES OF VPPA-WELDED 2090-T83 SHEET AT LOW TEMPERATURES FOR SEVERAL POST-WELD HEAT TREATMENTS (43, FIG. 4–7)

Alloy	2090-T83						
Specimen Machining	Welds Machined Flat					Tested as Welded	
Weld Process[a]	Variable Polarity Plasma Arc				GTA	VPPA	
Thickness, in.	0.12	0.12	0.21	0.32[b]	0.12	0.12	0.21
Postweld Heat Treat.	None	T62	None	None	None	None	None
Failure Location	Weld	HAZ	Weld	Weld	Weld	Weld	Weld
F_{tu}, ksi	35	64	37	36	36	45	42
F_{ty}, ksi	22	48	21	22	23	26	25
Elongation, percent	4.2	10	7	6	4.3	4	4

(a) Filler ER2319, except as noted; all welds vertical.
(b) Horizontal weld.

TABLE 4.0313. TENSILE PROPERTIES OF 2090-T83 SHEET WELDED BY VPPA AND GTA PROCESSES (42, TABLES 2 AND 3)

	Al
2.7	Cu
2.3	Li
0.12	Zr

2090 Al

Alloy	2090		2219	
Temper	T83		T851	
Form	0.25-in. Sheet		0.75-in. Plate	
Weld	None	VPPA[a]	None	VPPA
F_{tu}, ksi	84	42	68	40
F_{ty}, ksi	78	25	55	18
Elongation, percent	6	9	9	18

(a) Variable Polarity Plasma Arc with EB2319 filler.

TABLE 4.0314. COMPARISON OF PARENT METAL AND WELD METAL TENSILE PROPERTIES FOR 2090 SHEET AND 2219 PLATE (43, TABLE 2)

Alloy	2090
Temper	T83
Form	0.125-in. Sheet
Welds	Variable Polarity Plasma Arc With EB2319 Filler
Test Temperature, F	-423
F_{tu}, ksi	60
F_{ty}, ksi	37
Elongation, percent	2.4

TABLE 4.0315. TENSILE PROPERTIES AT CRYOGENIC TEMPERATURE FOR 2090-T83 SHEET WELDS (42, TABLE 5)

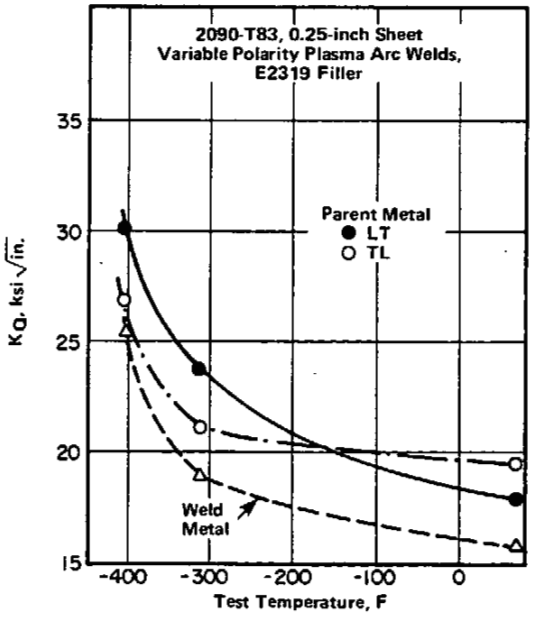

FIGURE 4.0316. FRACTURE TOUGHNESS AS FUNCTION OF LOW TEMPERATURES FOR PARENT METAL AND VPPA WELDS (43, FIGURE 3)

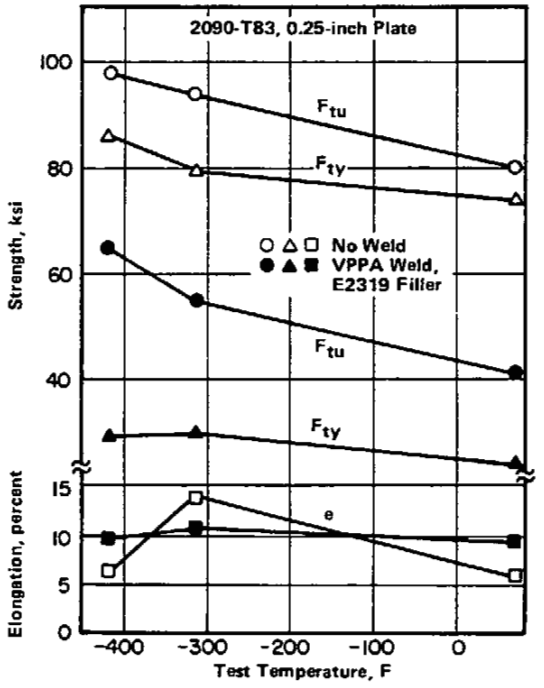

FIGURE 4.0317. TENSILE PROPERTIES OF WELDED AND UNWELDED 2090-T83 PLATE AS A FUNCTION OF TEMPERATURE (43)